4.2.2. GRAVITY AND GEOMAGNETIC FIELD OBSERVATIONS AND OUTCROP SAMPLING IN AREAS INSUFFICIENTLY COVERED BY PREVIOUS SURVEYS

4.2.2.1. Location of the field works

During the 2016 campaign, field activities (mainly gravity and magnetics along with sampling of major outcrops) were performed in several areas insufficiently covered by previous survey: Rodna-Bârgău and Northern Călimani Mts, Gurghiu Mts, and Northern Harghita Mts (Fig. 4.2.2.1). A few observations were also made in the Perşani Mts in order to clarify some local aspects.

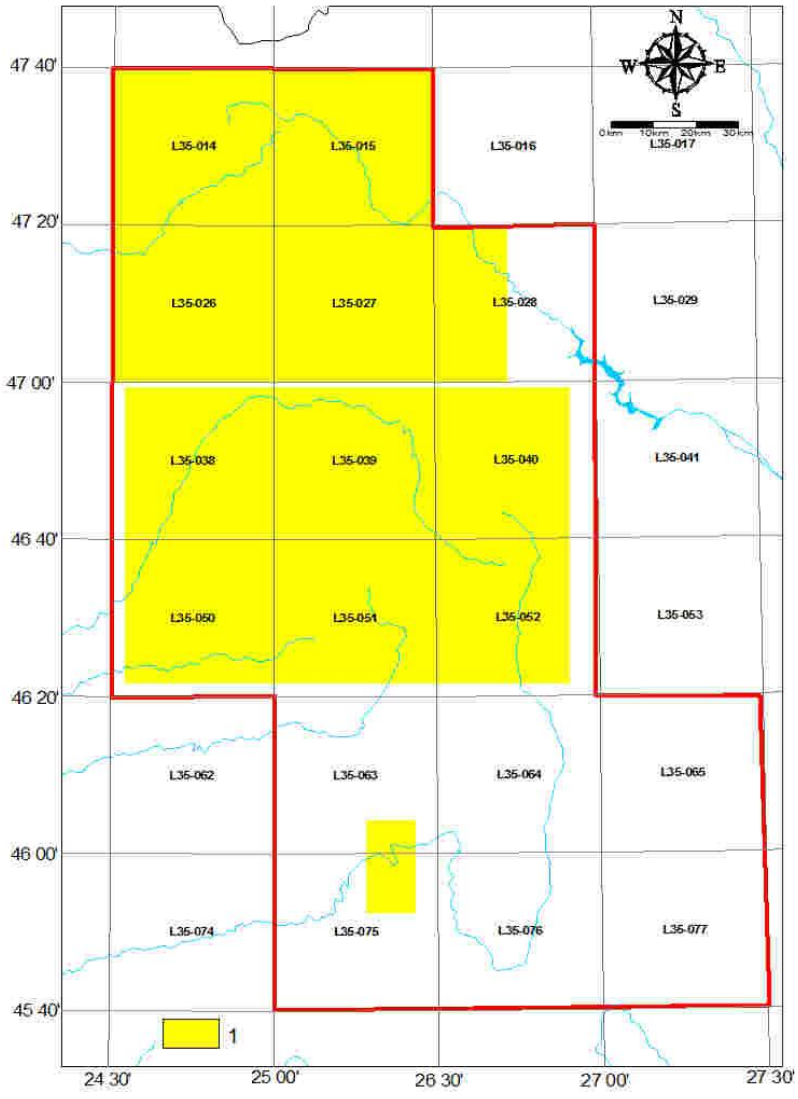

Fig. 4.2.2.1 Location of the field activities perormed during 2016
1, surveyed areas

4.2.2.2. Gravity

4.2.2.2.1. Instruments and methodology

A **Scintrex CG-5 AUTOGRAV meter** was employed for relative gravity observations within the studied areas. This is currently the most commonly used gravity meter worldwide. Technical specifications were presented in our previous reports.

Several ***auxiliary operations*** were performed prior and after the field campaign:

- checking up the calibration factor: has been conducted on the UNIGRACE calibration line Cluj Napoca - Beliş (172,12 mgal)

- checking up the drift factor: has been systematically performed in the underground gravity lab of the Solid Earth Dynamics Dept prior and after each field campaign

- absolute gravity transfer: has been achieved by designing and implementing special reference networks providing gravity ties to base stations belonging to the Romanian national gravity system or to European UNIGRACE network.

Field observations

Gravity observations have been performed in repeated measuring cycles based on several local base stations of the survey (e.g. Milsom & Eriksen , 2011; Hinze et al, 2013).

Fig. 4.2.2.2.1 Scintrex CG-5 AUTOGRAV run on a gravity station

Local reference base stations were located in the neighbourhood of the Lepşa and Topliţa base stations belonging to the second order national reference network.

4.2.2.2.2. Gravity data primary processing

The primary processing of gravity data are aimed at providing consistent data. The following corrections have been applied (e.g. Hinze et al., 2013):

- **instrumental reductions**
  - **-tide effect**
  - **-residual drift**
- **base reduction and computing the absolute gravity value**
- **theoretical gravity (latitude) reduction (Silva-Cassini, 1934)**
- **elevation reduction**
- **Bouguer plate reduction**
- **Bouguer correction**

The Bouguer anomaly resulting from the application of the above-mentioned corrections/reductions represents the difference between the effect of the real Earth and a theoretical one, with the same shape, but a homogeneous (unique) value of density.

In case of the INSTEC gravity survey, the Bouguer anomaly has been computed for the two standard densities formally used in the construction of the National Gravity Map of Romania: 2200 kg/m^3 and 2670 kg/m^3. Both may be equally employed, but correlations with the model of the observation surface have demonstrated that the last one (2670 kg/m^3) better mitigates the geometric effect of topography.

4.2.2.2.3. Gravity results within the investigated areas

4.2.2.2.3.1. Rodna-Bargau perimeter

Figure 4.2.2.2.2 shows location of gravity data points within the northern part of INSTEC area, the Rodna-Bârgău perimeter. These were added to complete the previously obtained information (Mocanu, Rădulescu, 1994).

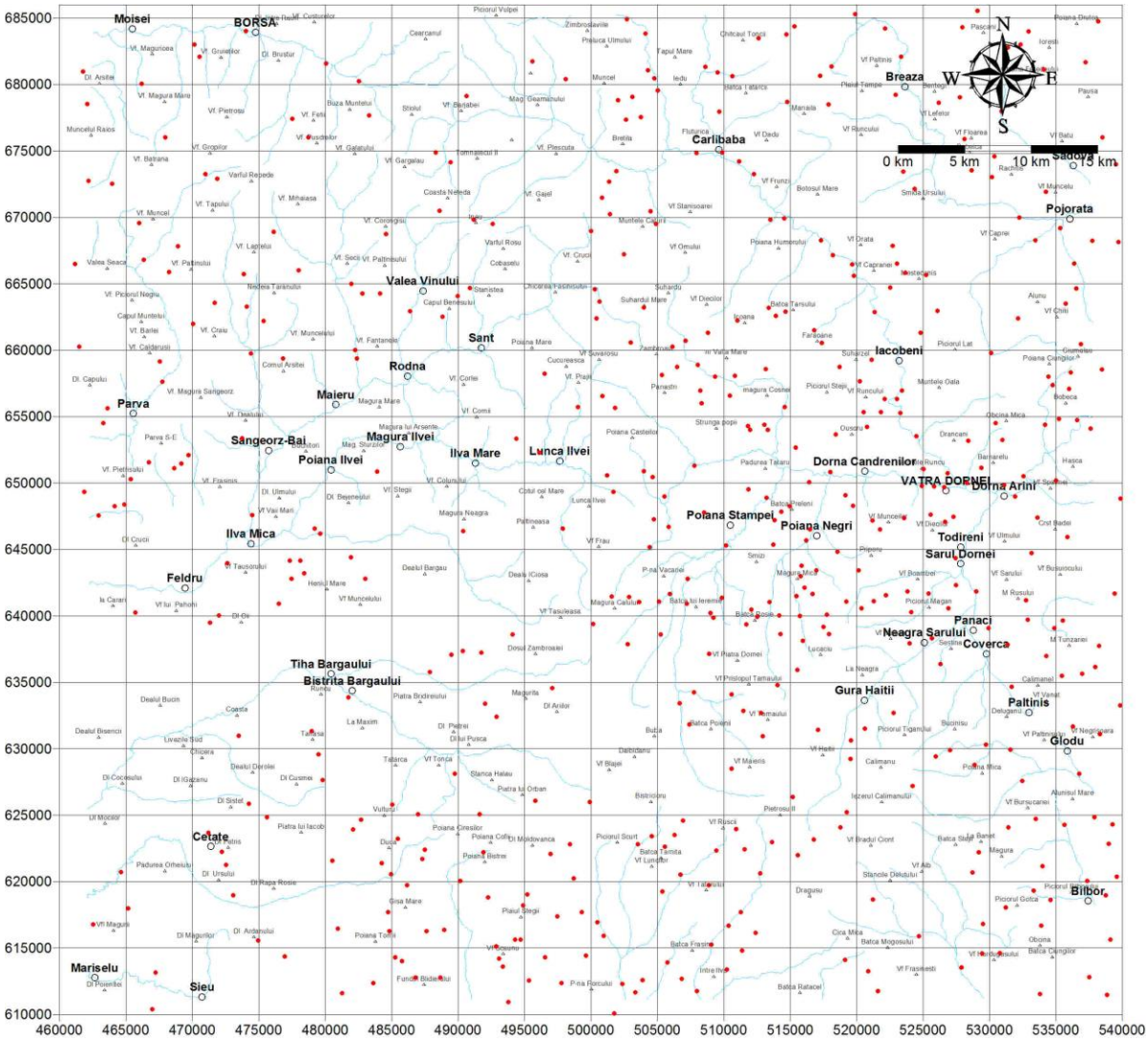

Fig. 4.2.2.2.2 Location of gravity datapoints within Rodna-Bârgău area

The obtained composite Bouguer anomaly map is shown in Figure 4.2.2.2.3. Correlation with topography is presented for the density of 2670 kg/m^3 in Figure 4.2.2.2.4.

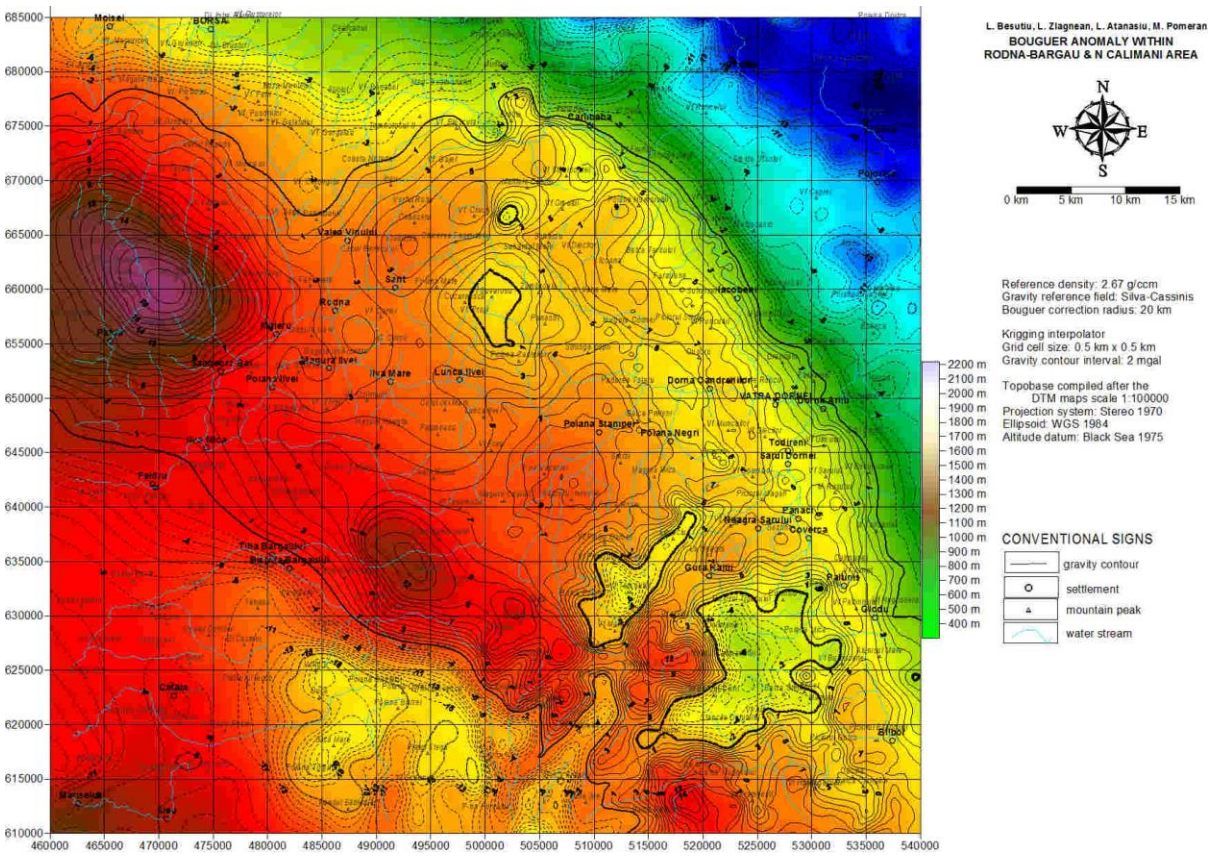

Fig. 4.2.2.2.3. Bouguer anomaly within the Rodna-Bârgău and North Călimani Mts area

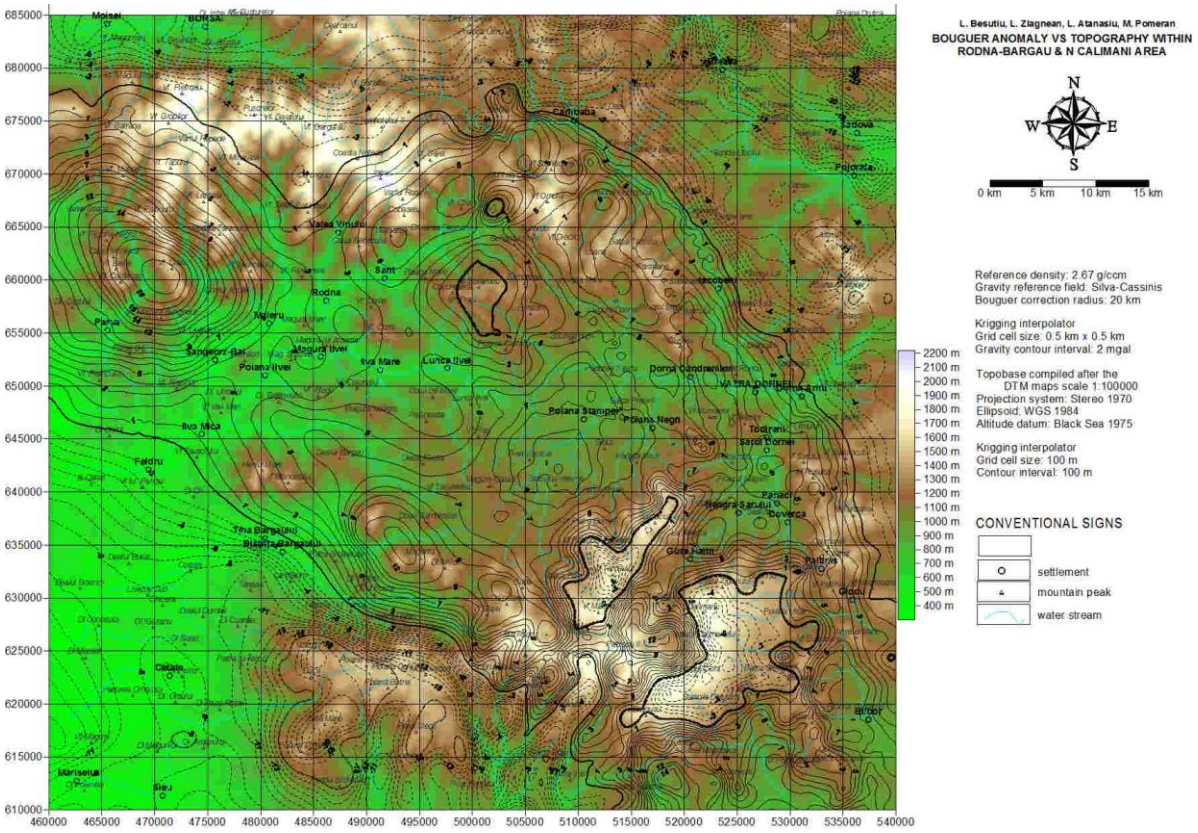

Fig. 4.2.2.2.3. Bouguer anomaly within the area Rodna-Bârgău and North Călimani Mts vs topography

4.2.2.2.3.1. Gurghiu perimeter

The second area surveyed in the 2016 campaign was the Gurghiu Mts and Northern Harghita Mts (Fig, 4.2.2.2.5).

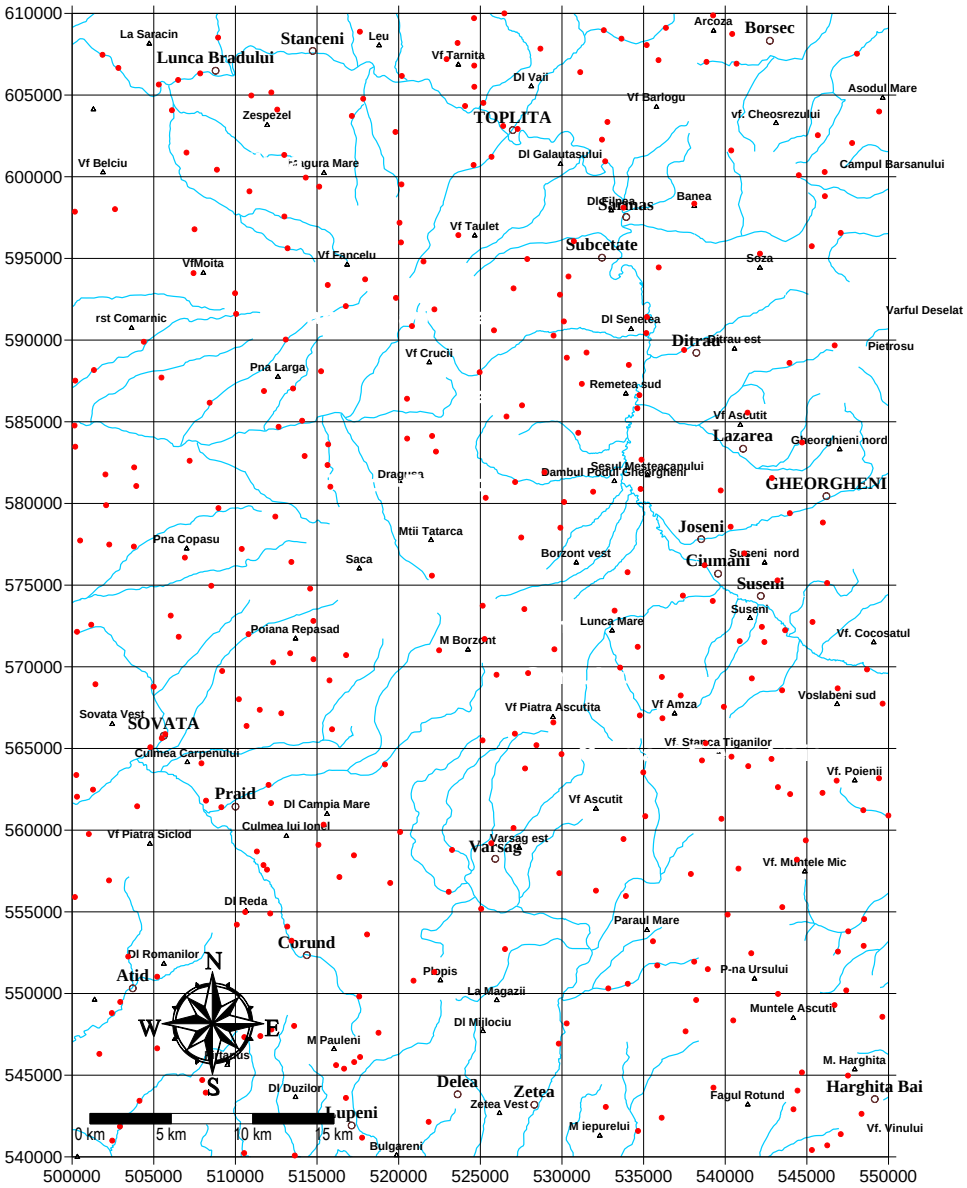

Fig. 4.2.2.2.4 Location of gravity data points in the Gurghiu Mts and N Harghita Mts area

Based on the integration of the newly gathered data with previous information (Mocanu, Rădulescu, 1994) a composite Bouguer anomaly map has been constructed for the reference density of 2670 kg/m^3 (Fig. 4.2.2.2.5).

A brief analysis on the appropriateness of that value is presented by Figure 4.2.2.2.6 .

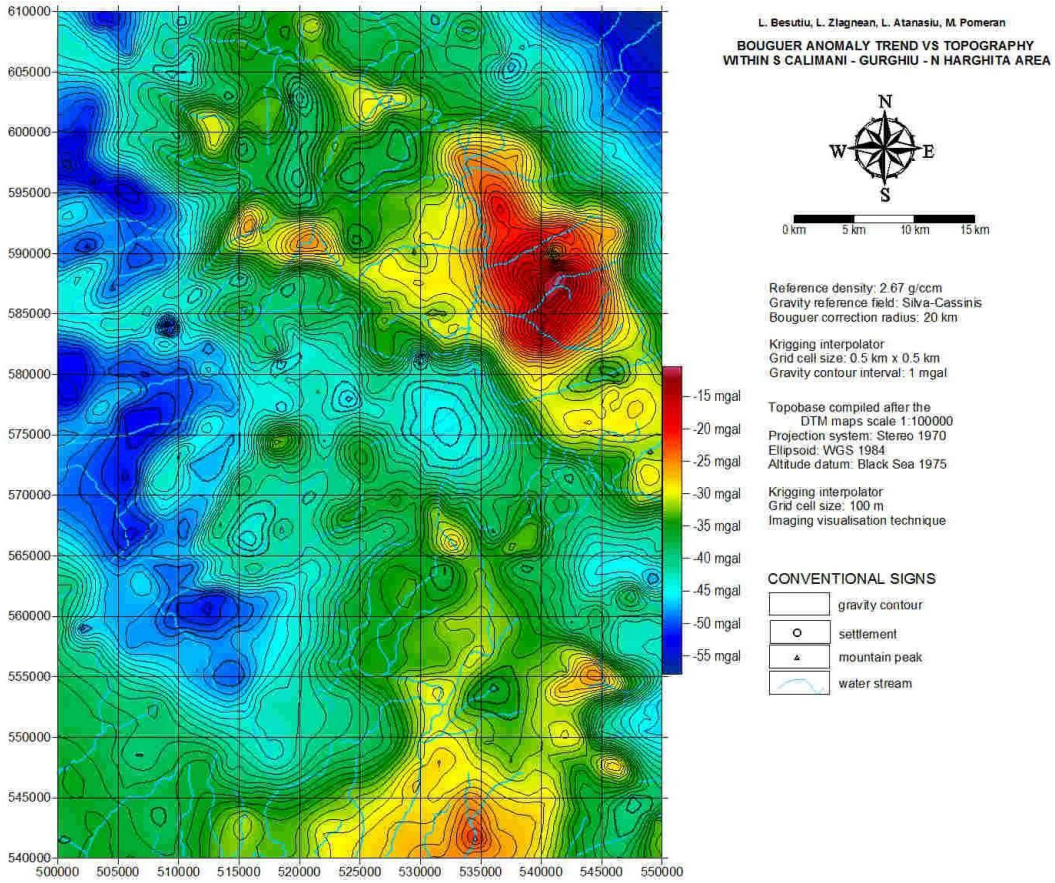

Fig. 4.2.2.2.5. Bouguer anomaly in the Gurghiu Mts and N Harghita Mts

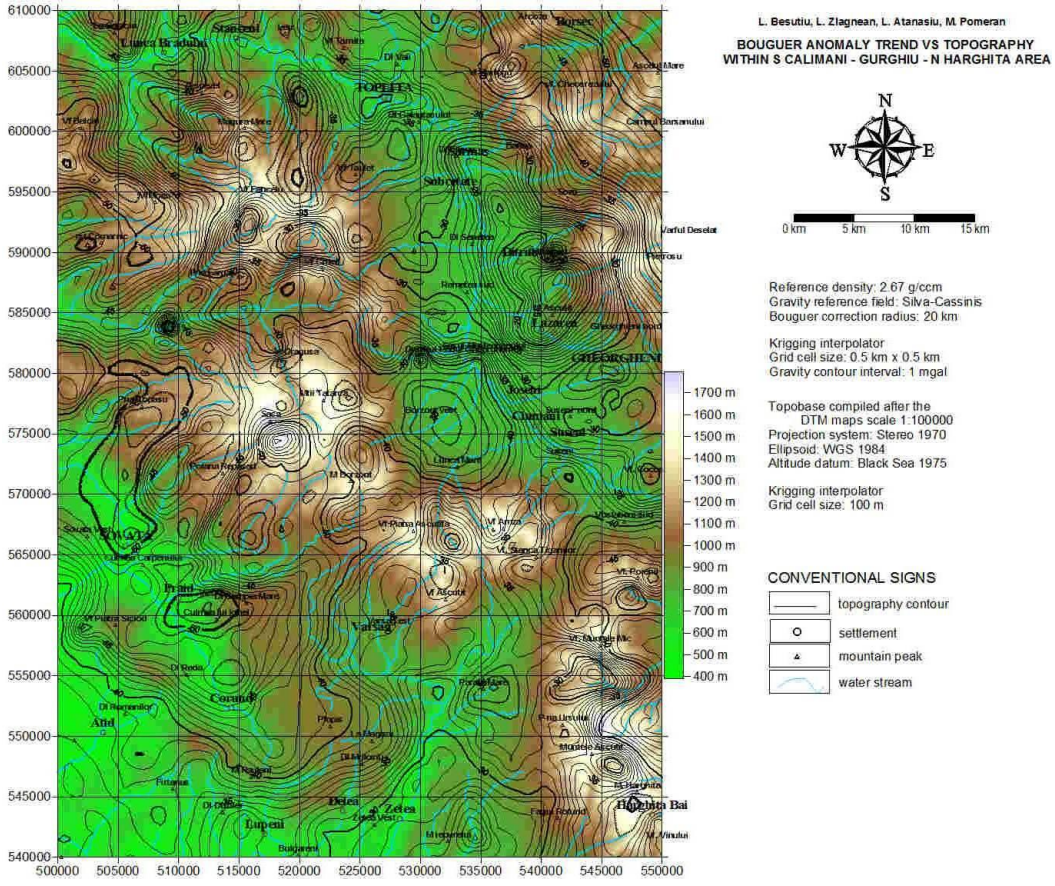

Fig. 4.2.2.2.6. Bouguer anomaly in the Gurghiu Mts and N Harghita Mts area vs. topography

4.2.2.3. Ground magnetics

4.2.2.3.1. Instruments and methodology

Unlike gravity exploration, ground magnetics require at least two instruments working simultaneously: one in the field and the other in the base station for removing diurnal activity effects. A **Geometrics G856 AX proton magnetometer** has been used for current field observations. A **Scintrex SM-5 NAVMAG optical pump magnetometer** was used for diurnal activity recording in the base station.
Given the capability of magnetometric instrumentation to observe absolute values of geomagnetic field, the survey is much simplified. Figure 4.2.2.3.1 shows the G856 AX run in a field station. As it can be observed, especially in mountain areas, it needs a team of two workers: one carrying the sensor, and the other the central unit.
Data point locations have been obtained with a handheld Garmin GPS.

Fig. 4.2.2.3.1 Geometrics G856 AX run along an observational line

4.2.2.3.2. Data processing

Standard primary data processing has been performed (Reeves, 2005; Milsom & Eriksen , 2011) by applying the following reductions:

- **diurnal activity**
- **base reduction**

Geomagnetic anomaly

The geomagnetic anomaly (ex. Reeves, 2005; Hinze et al, 2013**)** has been computed by subtracting a reference geomagnetic field from the geomagnetic observations field. The reference geomagnetic field represents the effect of the main geomagnetic field generated by electrical currents located at the outer part of nucleus at the contact with lower mantle. To remove these planetary effects, the IGRF 12 model (Thebault et al, 2015) has been applied.

4.2.2.3.3. Geomagnetic anomalies in the areas surveyed in 2016

4.2.2.3.3.1. Rodna-Bârgău perimeter

Figure 4.2.2.3.3.1 shows location of the additional geomagnetic data points obtained during the 2016 field campaign.

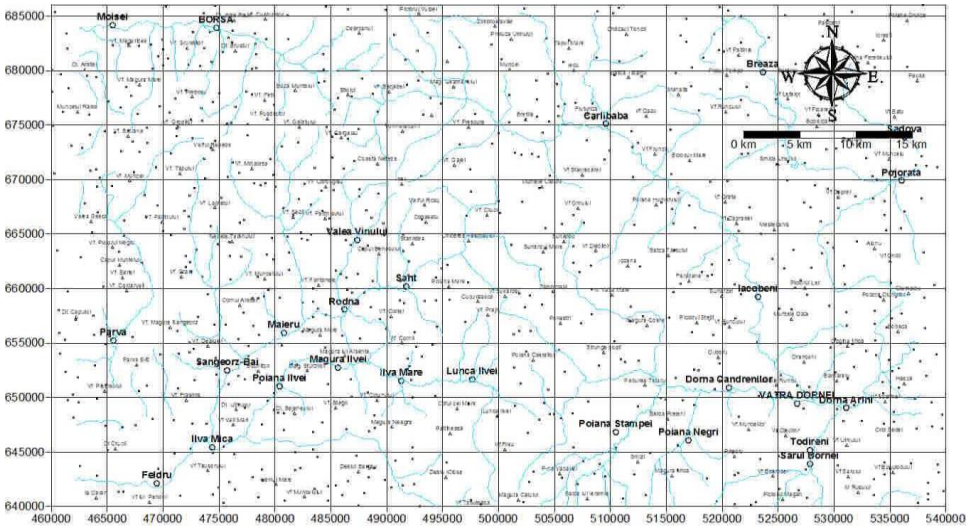

Fig. 4.2.2.3.3.1 Location of geomagnetic data points observed within 2016 field survey

A homogeneous set of data has been then obtained through the integration of our observations with previously collected geomagnetic data. Based on this data set, consistent geomagnetic images have been obtained. To avoid the noisy geometric effect of topography, data were upward continued on a plan situated above the highest altitude in the area (Fig. 4.2.2.3.3.2).

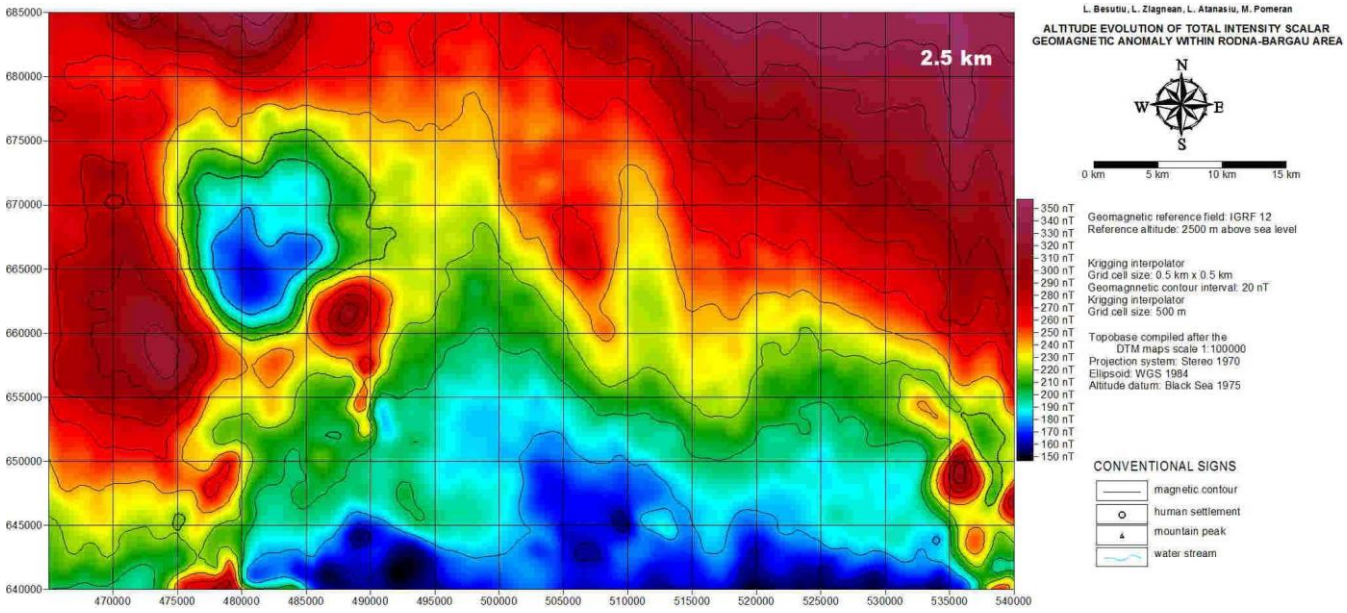

Fig. 4.2.2.3.3.2. Geomagnetic anomaly within Rodna-Bârgău area

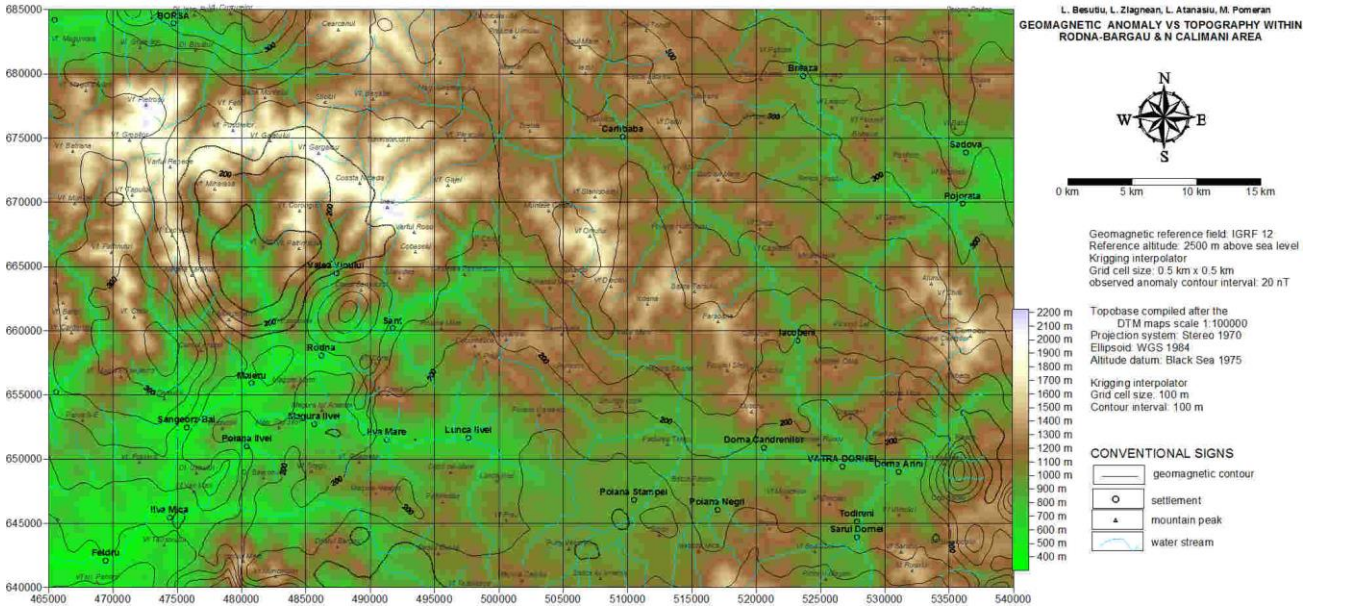

Fig. 4.2.2.3.3.3. Geomagnetic anomaly within Rodna-Bârgău area vs. topography

4.2.2.3.3.2. Gurghiu perimeter

New data were collected in order to complete the regional information previously obtained in the area. New data point locations for geomagnetic observations in the Gurghiu Mts are presented in figure 4.2.2.3.3.4.

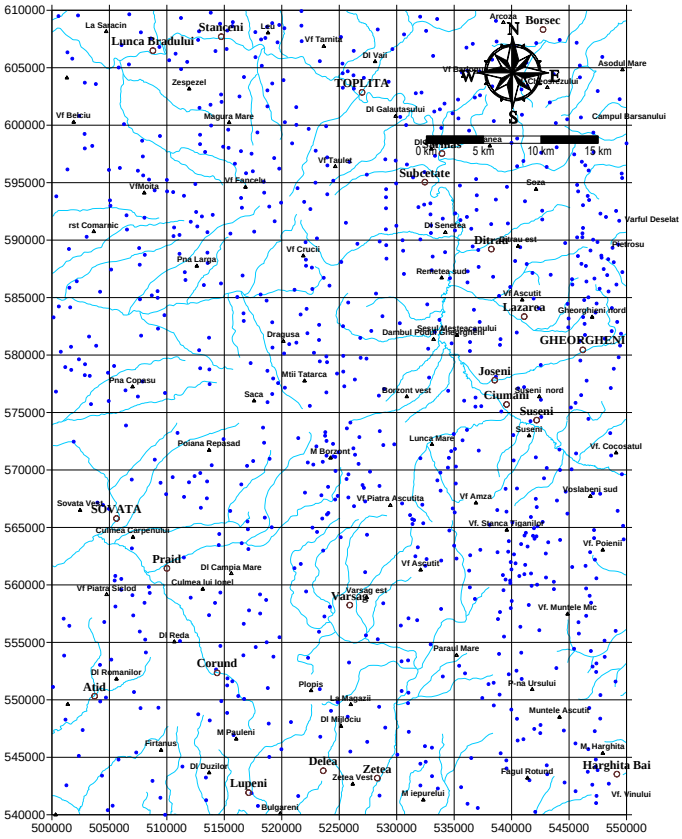

Fig. 4.2.2.3.3.4. Location of the geomagnetic data points achieved in the Gurghiu Mts and N Harghita Mts during the 2016 field survey.

A homogeneous data set has been obtained by the integration of new observations with previous geomagnetic data. Based on the updated data set, consistent geomagnetic images have been obtained (Fig. 4.2.2.3.3.5). To avoid the noisy geometric effect of topography, data were upward continued on a plan above the highest altitude in the area (2200 m above the sea level).

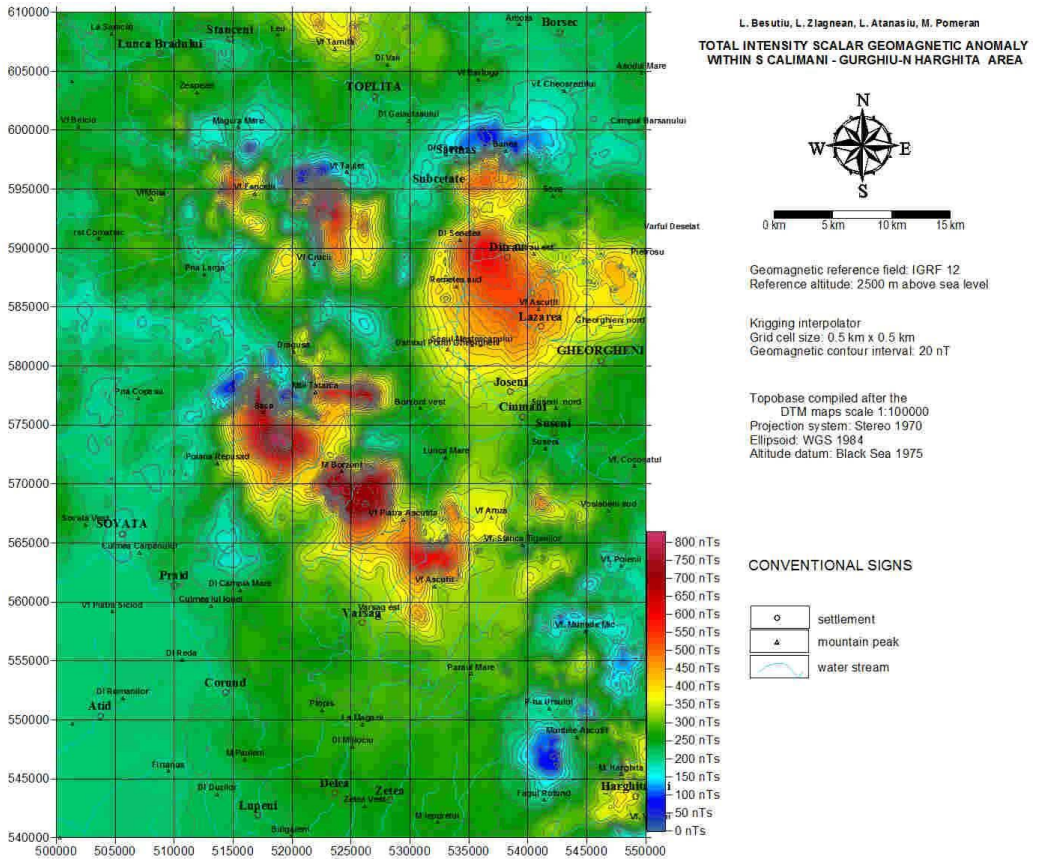

Fig. 4.2.2.3.3.4. The geomagnetic anomaly in the Gurghiu Mts and N Harghita Mts area

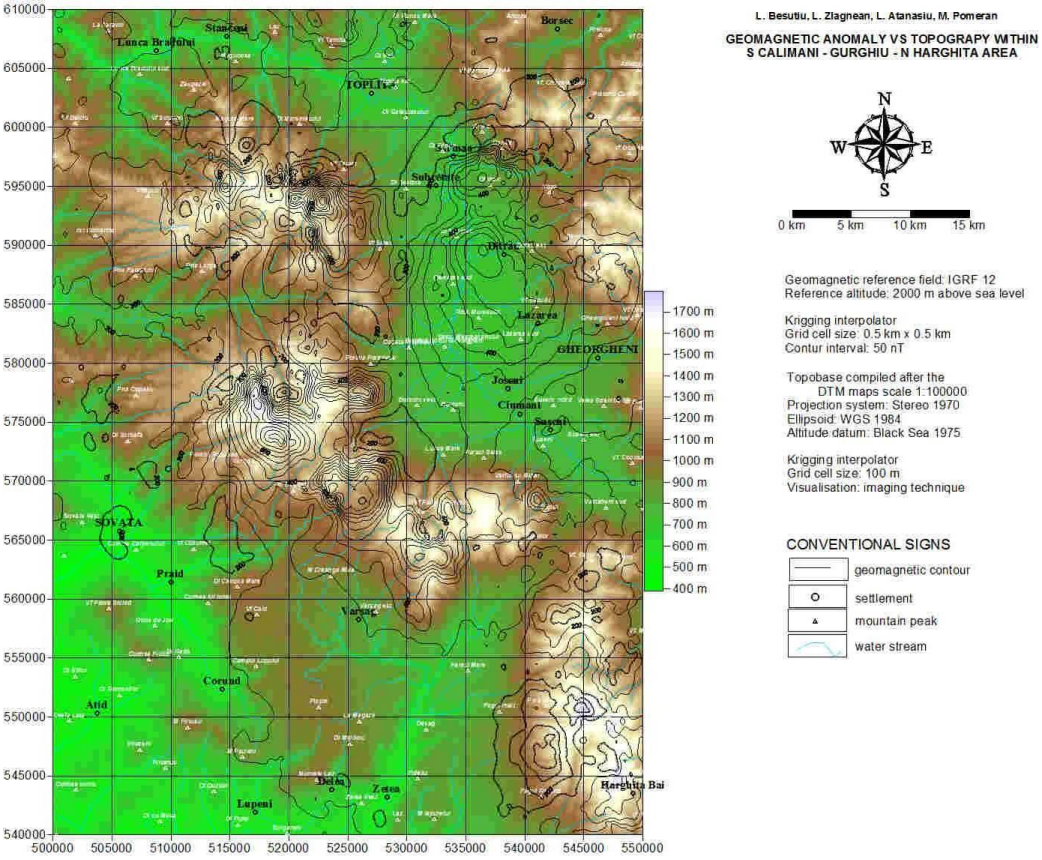

Fig. 4.2.2.3.3.5. The geomagnetic anomaly vs. topography in the Gurghiu Mts and N Harghita Mts area

4.2.2.4. Rock sampling

Sampled outcrops of the 2016 field campaign were limited to the northernmost part of the INSTEC area. Figure 4.2.2.4.1 shows location of the sampled outcrops.

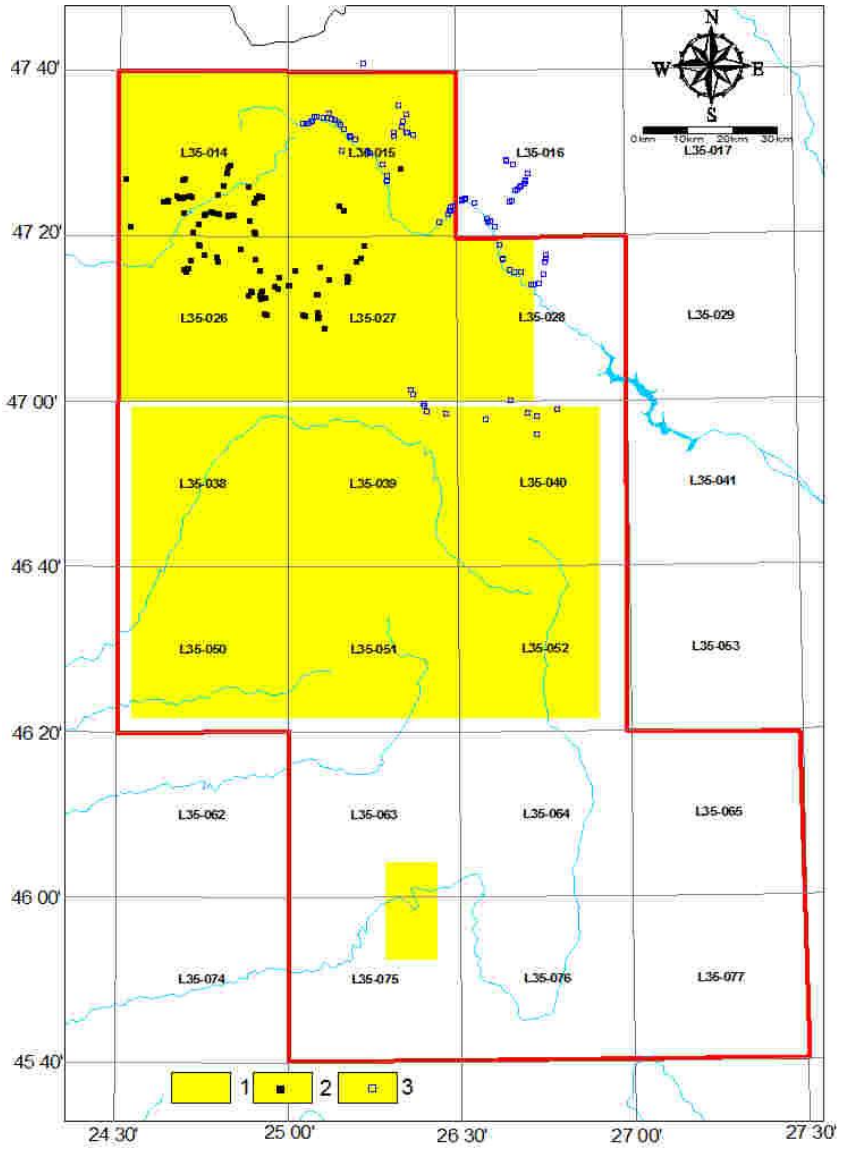

Fig. 4.2.2.4.1 Location of the sampled outcrops

1, areas covered by geophysical works during 2016; 2, outcrops sampled by the geology team, with absolute age dating 3, oucrops sampled by the geophysics team

Large outcrops (Fig. 4.2.2.4.2) have been chosen and thoroughly investigated through in situ measurements of magnetic susceptibility by using a Czech kappameter KT-5 provided by Ukrainian colleagues from the Institute of Geophysics of the Ukrainian National Academy of Sciences in Kiev.

Fig. 4.2.2.4.1 Outcrop magnetic investigation and sampling

Kappametric observations have been preferably performed on regular planar surfaces with no significant weathering phenomena and statistically considered (fig. 4.2.2.4.2). Following the observations, rock samples have been extracted from outcrops with unusual geomagnetic behaviour.

Fig. 4.2.2.4.2 Dr. Mykhailo Orlyuk with the Instiute of Geophysics, National Academy of Sciences of Ukraine, probing magnetic susceptibility on an outcrop

4.2.3. ADVANCED GEOPHYSICAL DATA PROCESSING; GENERATING NUMERICAL MODELS FOR ANOMALOUS SOURCES; UNRAVELING HIDDEN STRUCTURAL ELEMENTS

4.2.3.1. General considerations

Advanced data processing is aimed at offering more intuitive images, helping the interpreter to decipher their geological background. The processing is mainly performed by applying specially designed filters able to improve the signal/noise ratio by emphasising information followed by the researcher. To simplifu the mathematics behind the approach, more complicated when dealing with data in the spatial domain, most of this filtering operators are designed and applied in the frequency domain (e.g. Blakely, 1995, Brodie R.C., 2002, Reeves C., 2005).

The OASIS software packages that we have used for applying various filtering operators to our data (such as upward/downward continuation, reduce-to-pole geomagnetic anomaly, horizontal/vertical gradient, apparent magnetic susceptibility, pseudo-gravity, computation of regional/residual anomalies, etc.) are mainly working in the frequency domain by using Fast Fourier Transform (FFT) algorithm. FFT is used for both transferring space data into frequency domain and back in order to be exploited.

A special operator is the average power spectrum. It may be computed for both gravity and geomagnetic data and provides valuable information on the energy of the gravity and geomagnetic field in the studied areas. It is also useful in estimating the depth to the major contrasts of the rock physical properties (such as density or magnetic susceptibility) potentially useful in data modelling and interpretation.

In the followings, we shall present the results of advanced processing of the geomagnetic and gravity data gathered during the 2016 field campaign.

4.2.3.2. Filtered maps of the gravity and geomagnetic field in the areas investigated in 2016

4.2.3.2.1. Filtered images of the geomagnetic field

Fig. 4.2.3.2.1.1 presents the reduce-to-pole geomagnetic anomaly in the Rodna-Bârgău area.

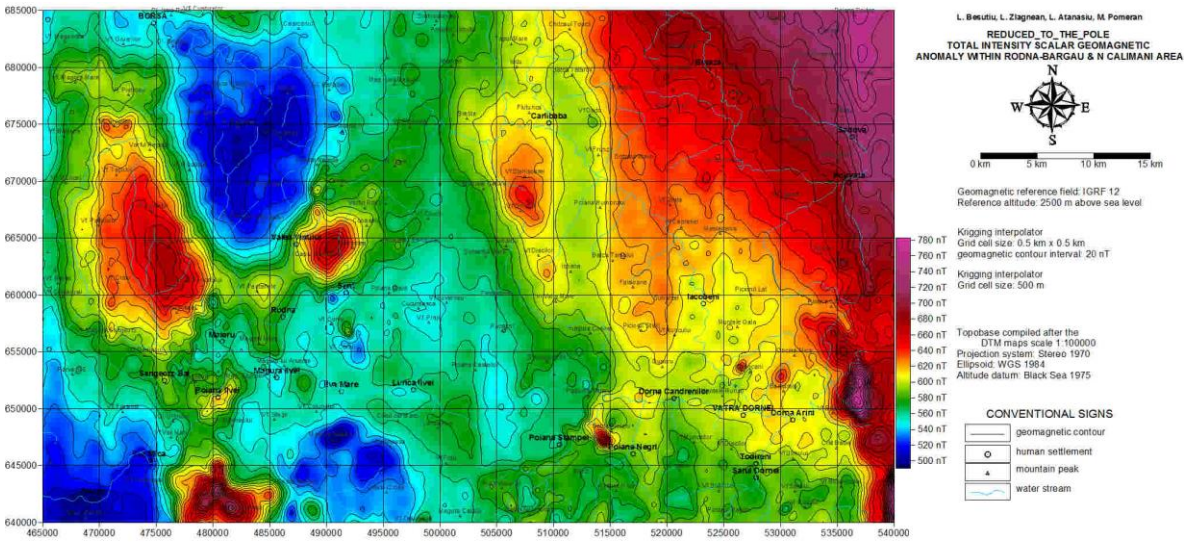

Fig. 4.2.3.2.1.1 Reduced-to-pole geomagnetic anomaly in the Rodna-Bârgău area

A comparative view with the former geomagnetic anomaly shows small differences only (fig. 4.2.3.2.1.2) in the location of the local anomalies due to the high value of the inclination and small value of declination of the polarising field in our country.

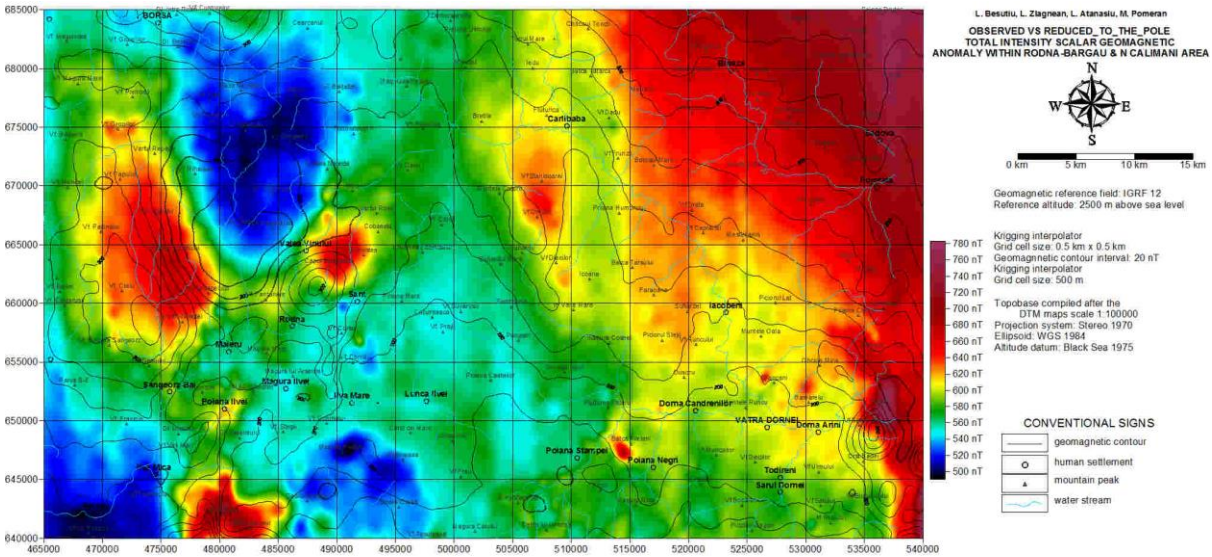

Fig. 4.2.3.2.1.2 Observed vs. reduced-to-pole geomagnetic anomaly in the Rodna-Bârgău area

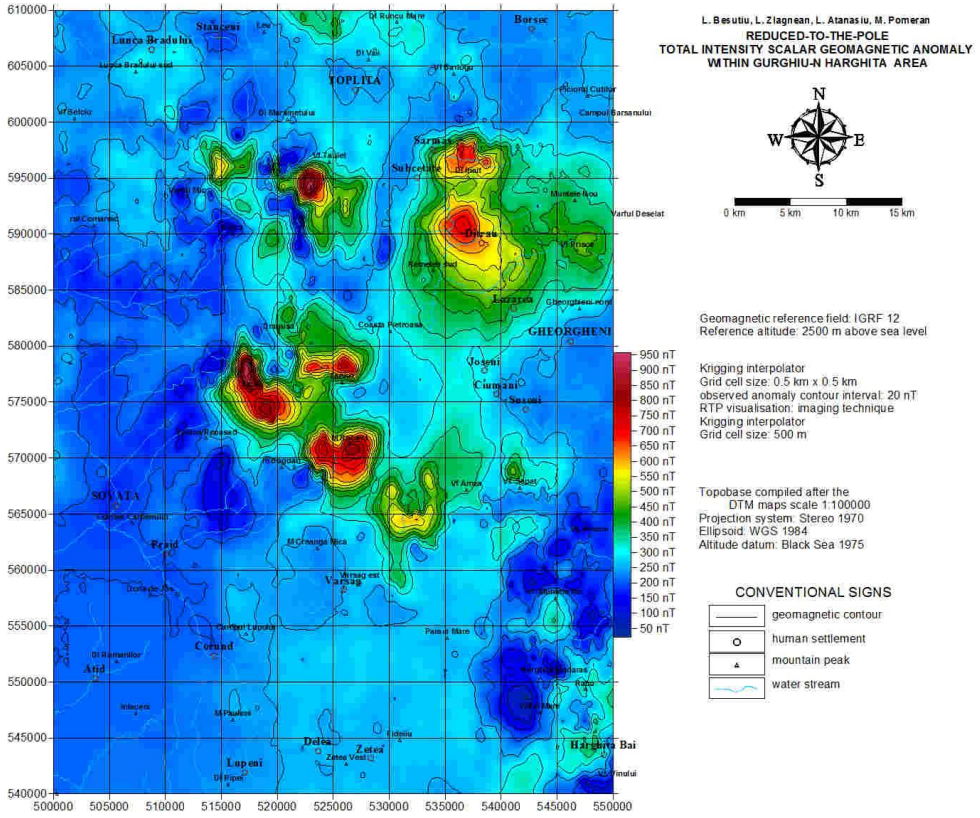

Fig. 4.2.3.2.1.3 Geomagnetic anomaly in the Gurghiu area

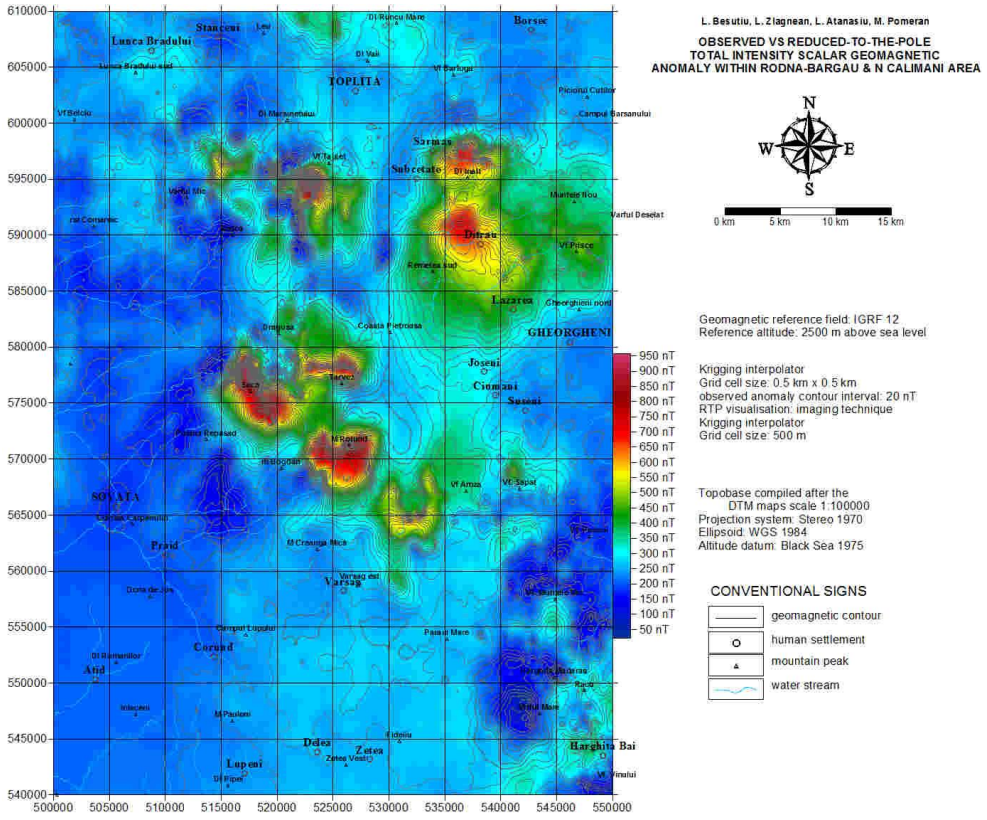

Fig. 4.2.3.2.1.4 Observed vs reduced-to-pole geomagnetic anomaly in the Gurghiu area

Fig. 4.2.3.2.1.5 shows vertical gradient and 4.2.3.2.1.6 the horizontal gradient of the geomagnetic anomalies in the Rodna-Bârgău area.

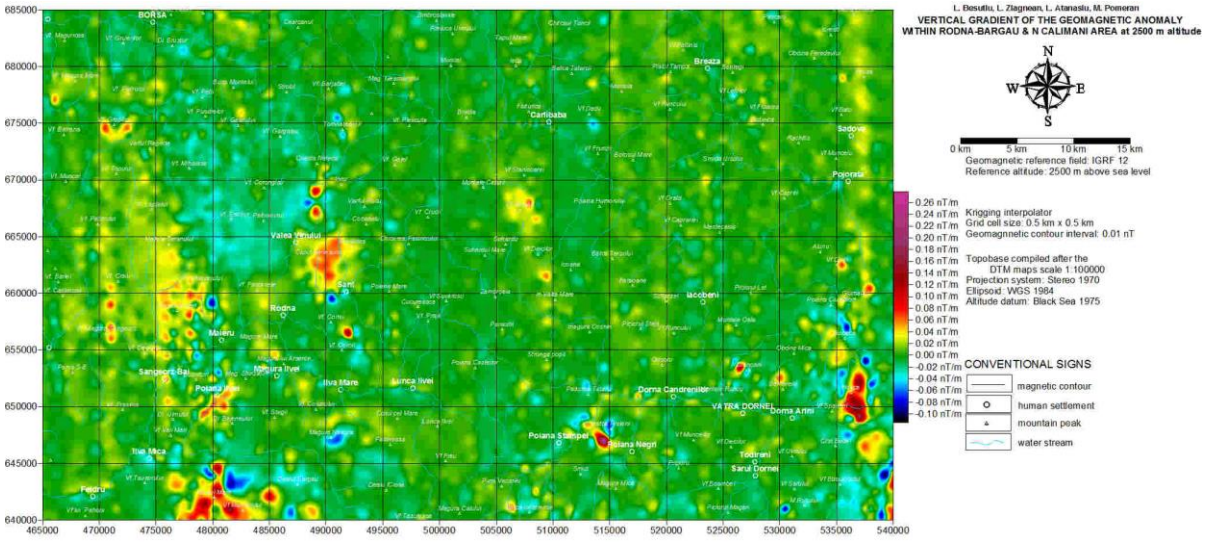

Fig. 4.2.3.2.1.5 Vertical gradient of the geomagnetic field in the Rodna-Bârgău area

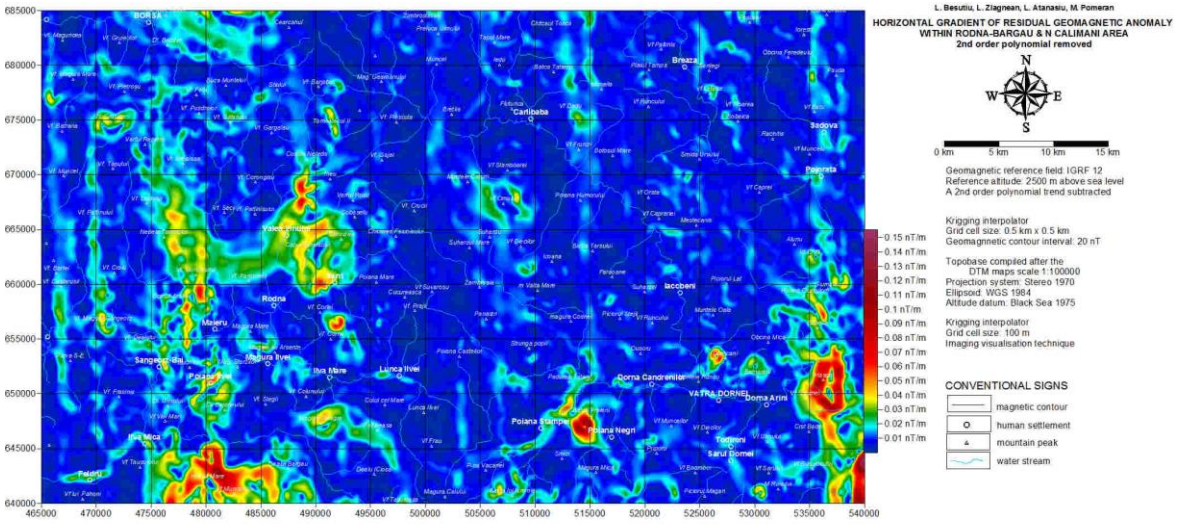

Fig. 4.2.3.2.1.5 Reduce-to-pole horizontal gradient of the geomagnetic field in the Rodna-Bârgău area

Both images are difficult to interpret due to high levels of noise introduced by metrology and inconsistency present among various categories of raw data.

Therefore, in the attempt to separate geomagnetic sources, various regional trends have been identified and removed from the observations. Also, the upward continuation allows for emphasizing the effect of deep/regional sources.

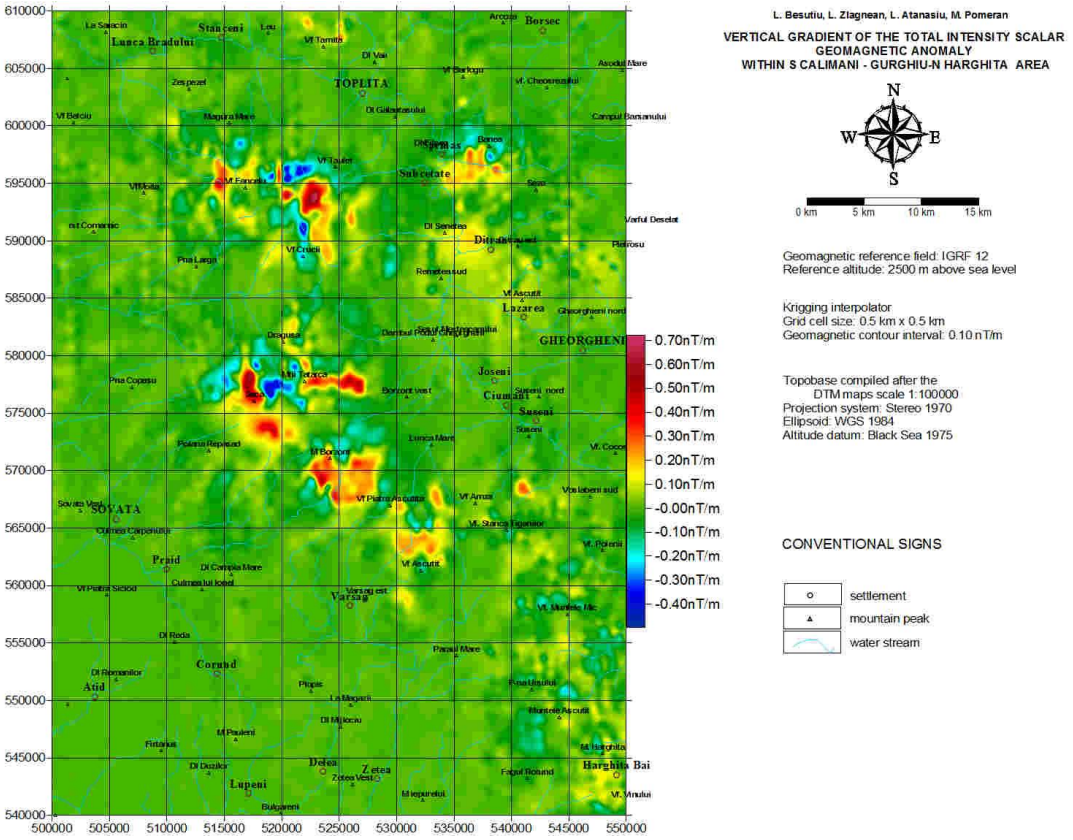

Fig. 4.2.3.2.1.6 Vertical gradient of the geomagnetic field in the Gurghiu area

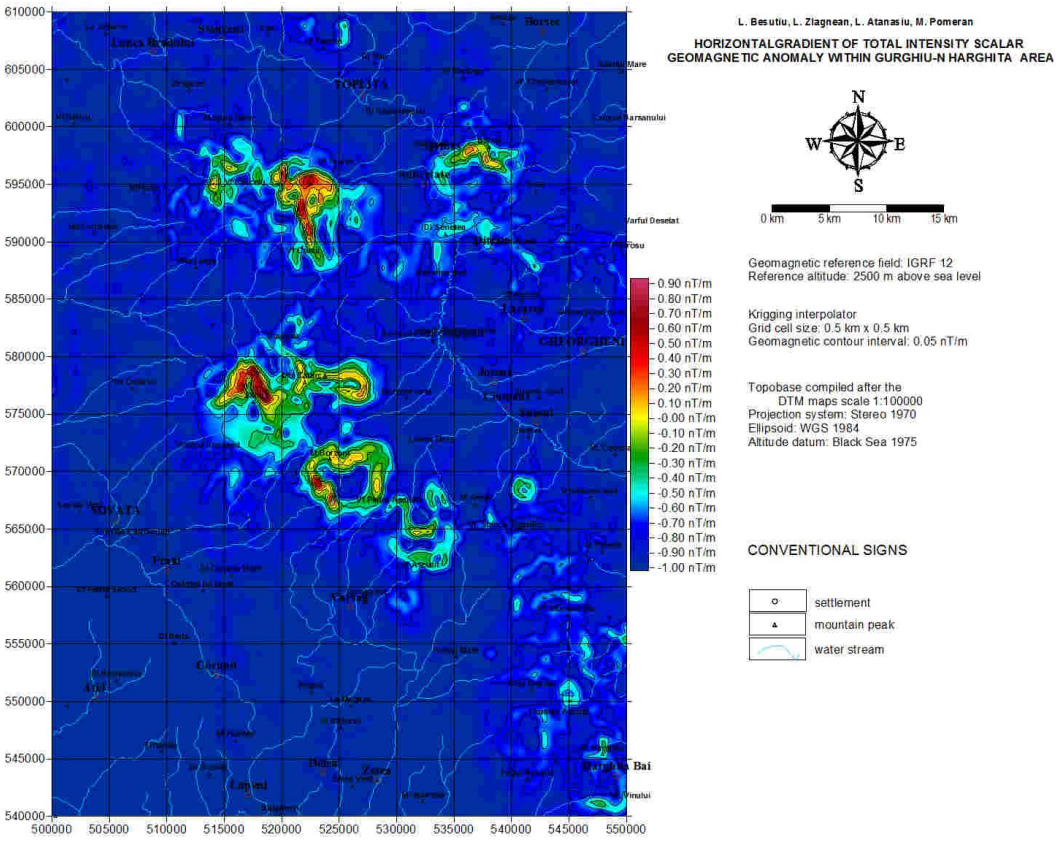

Fig. 4.2.3.2.1.7 Horizontal gradient of the geomagnetic field in the Gurghiu area

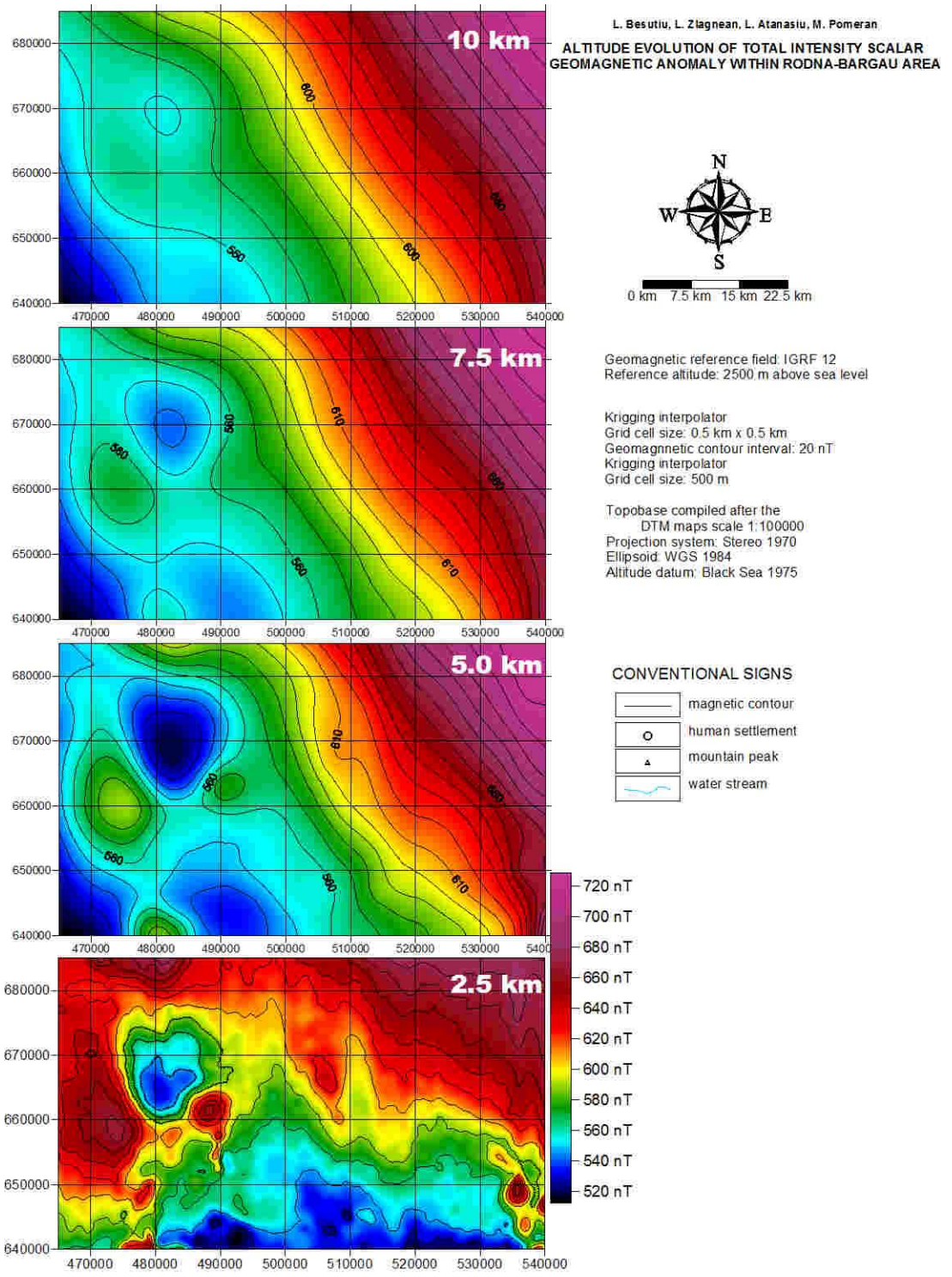

Fig. 4.2.3.2.1.8 Geomagnetic anomaly transferred on plans situated at various altitudes in the Rodna-Bârgău area

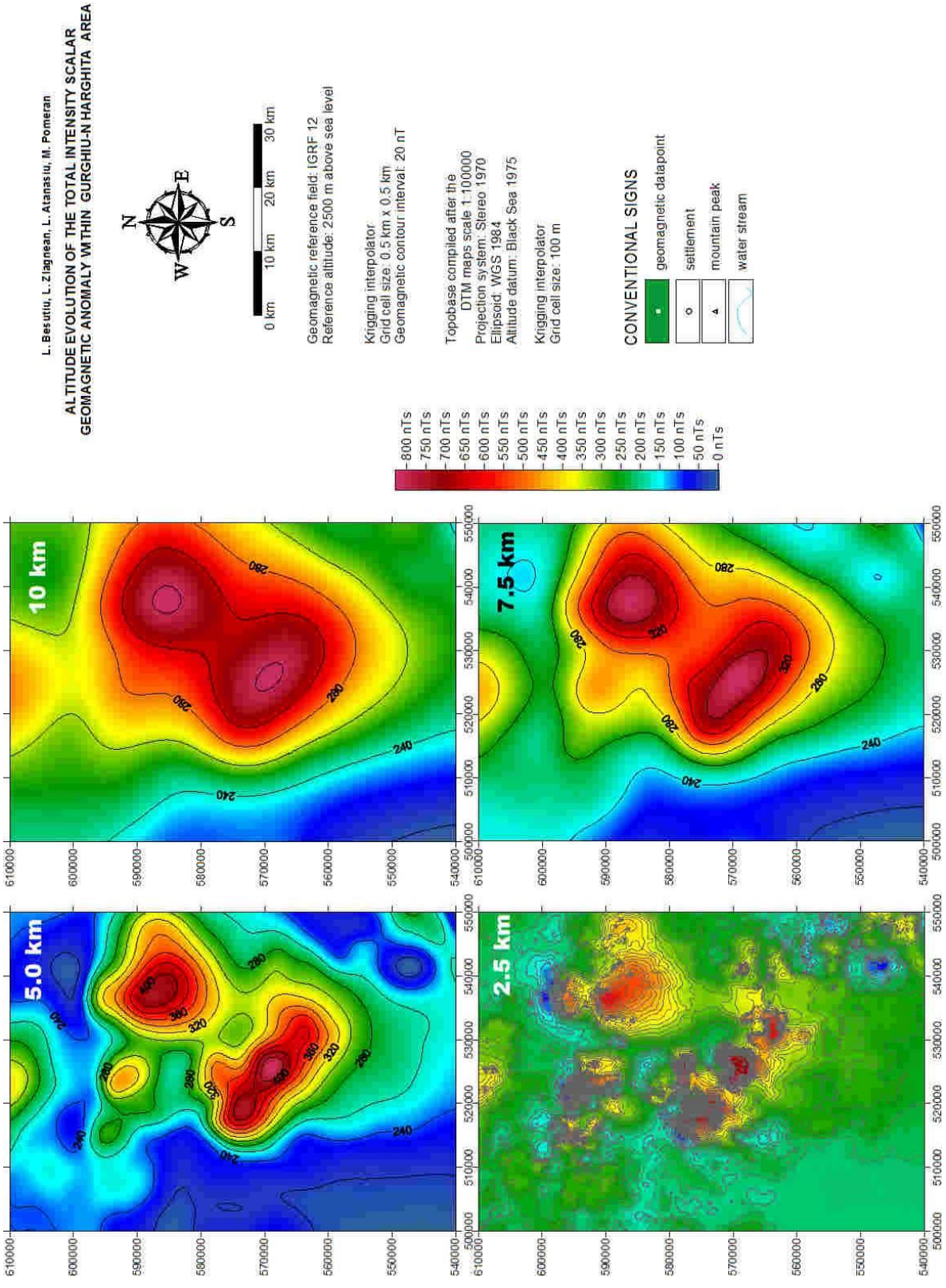

Fig. 4.2.3.2.1.9 Geomagnetic anomaly transferred on plans situated at various altitudes in the Gurghiu area

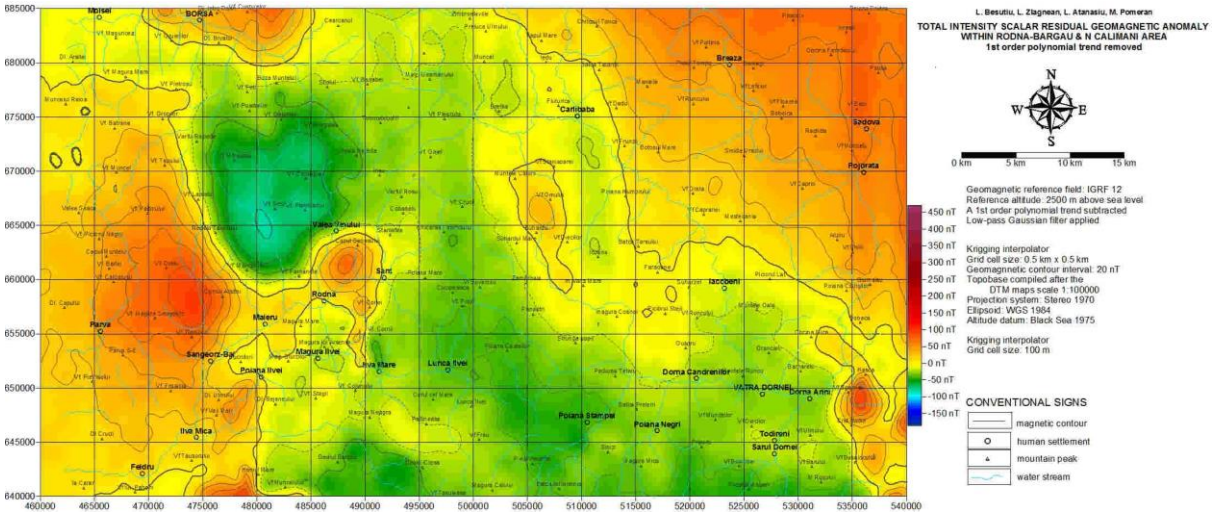

Fig. 4.2.3.2.1.10 Residual geomagnetic anomaly obtained by removing a first order polynomial trend from data

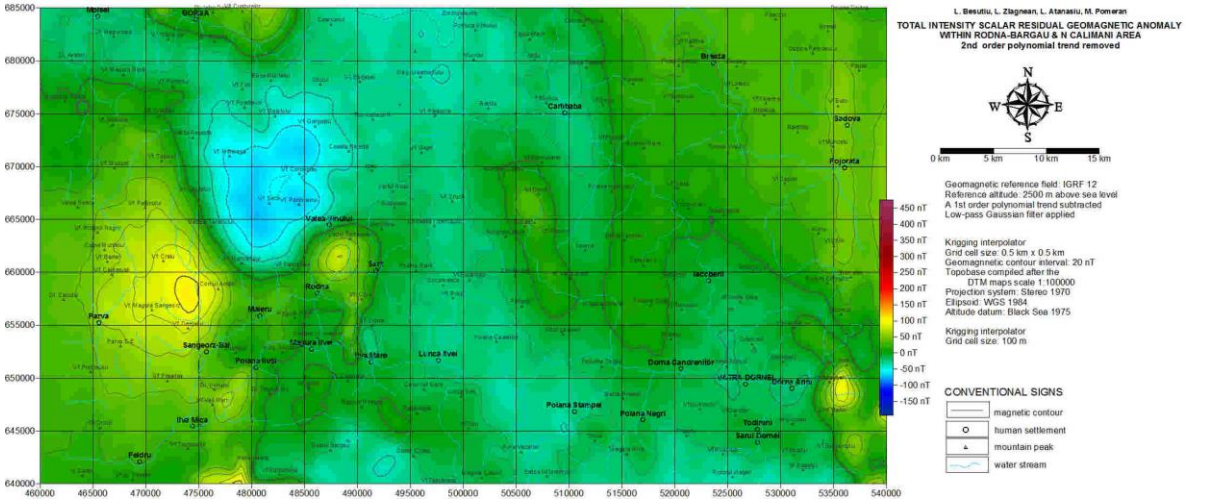

Fig. 4.2.3.2.1.11 Residual geomagnetic anomaly obtained by removing a second order polynomial trend from data

The analysis of the results obtained shows that the second order polynomial provides a the most balanced geomagnetic anomaly, within which lateral effects like the regional geomagnetic anomaly from Transylvanian Basin to the west, and the large Brodina-Bicaz effect to the east, are adequately controlled. Therefore, for other applied filters it was this residual to be taken into consideration instead of the raw anomaly.

Similar results have been obtained for the Gurghiu area (Figures 4.2.3.2.1.12 and figure 4.2.3.2.1.13).

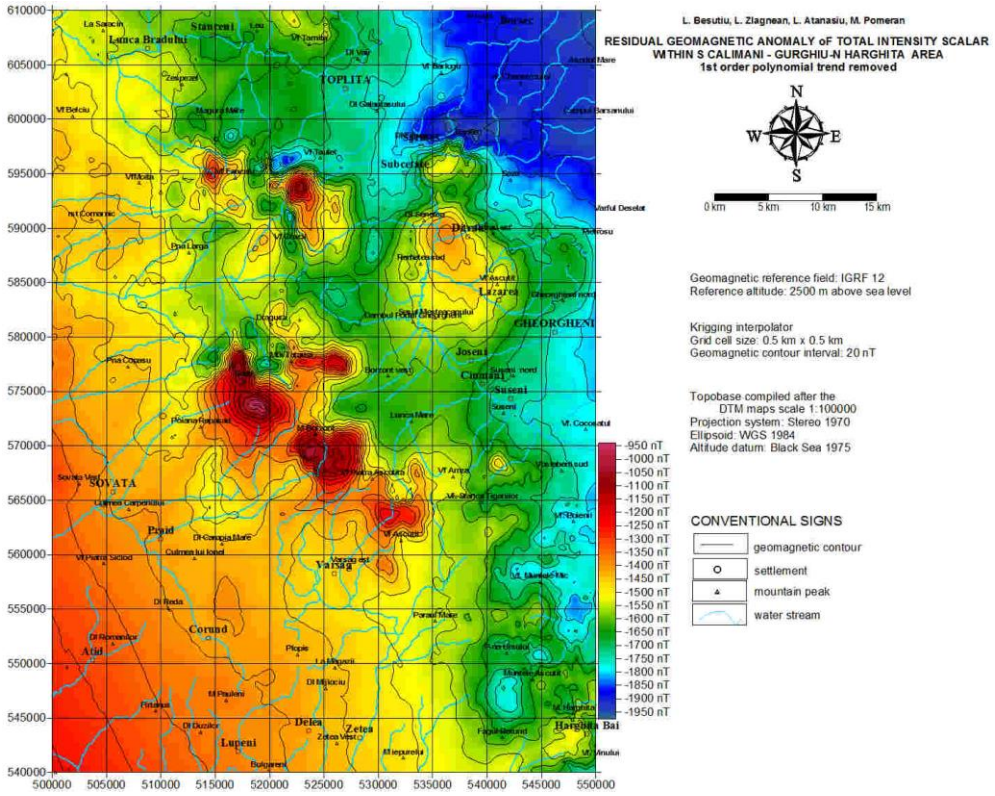

Fig. 4.2.3.2.1.12 Residual geomagnetic anomaly obtained by removing a first order polynomial trend from data

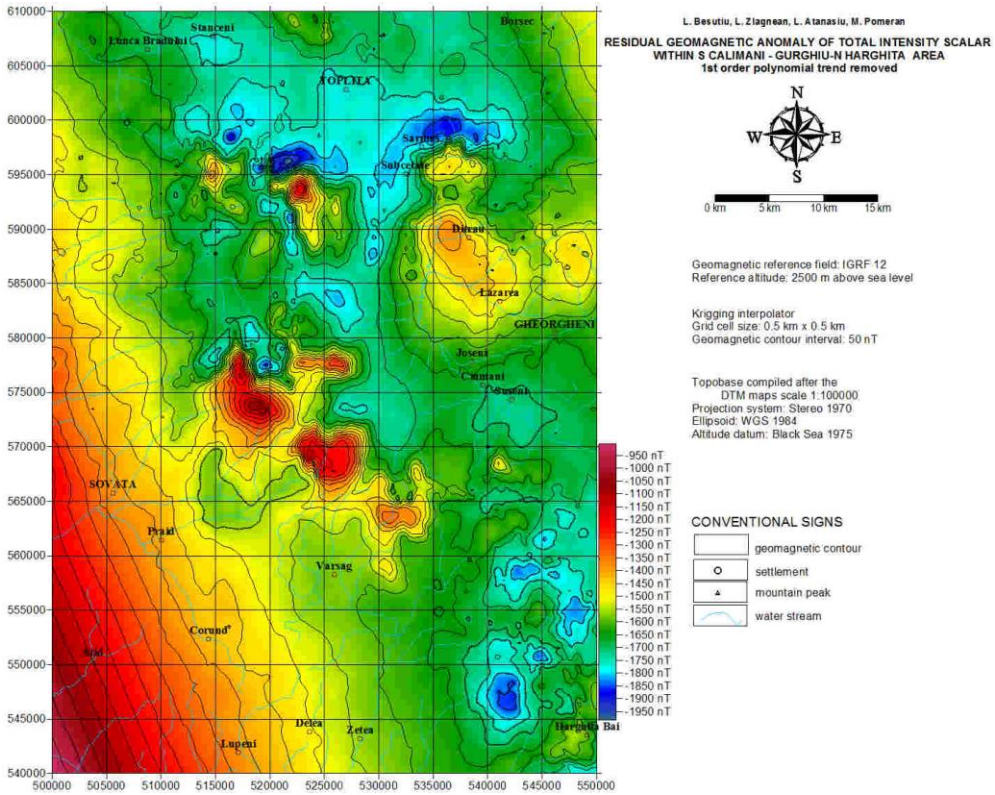

Fig. 4.2.3.2.1.13 Residual geomagnetic anomaly obtained by removing a second order polynomial trend from data

The next figures present the results of other three filtering operators: **analytical signal, apparent magnetic susceptibility and pseudo-gravity anomaly.**

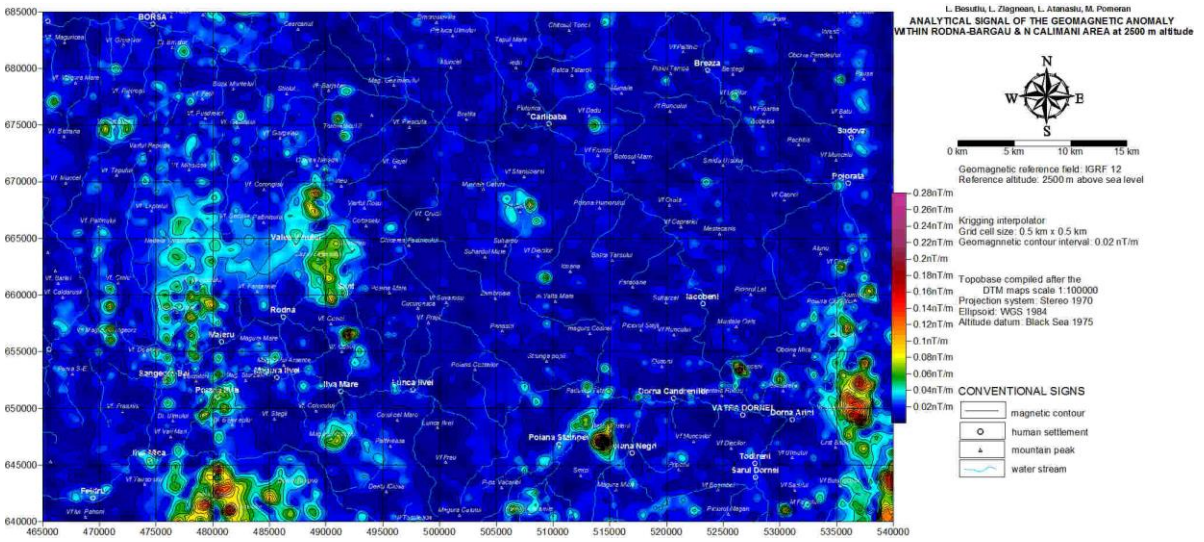

Fig. 4.2.3.2.1.14 Analytical signal of the reduced-to-pole geomagnetic anomaly in Rodna-Bârgău

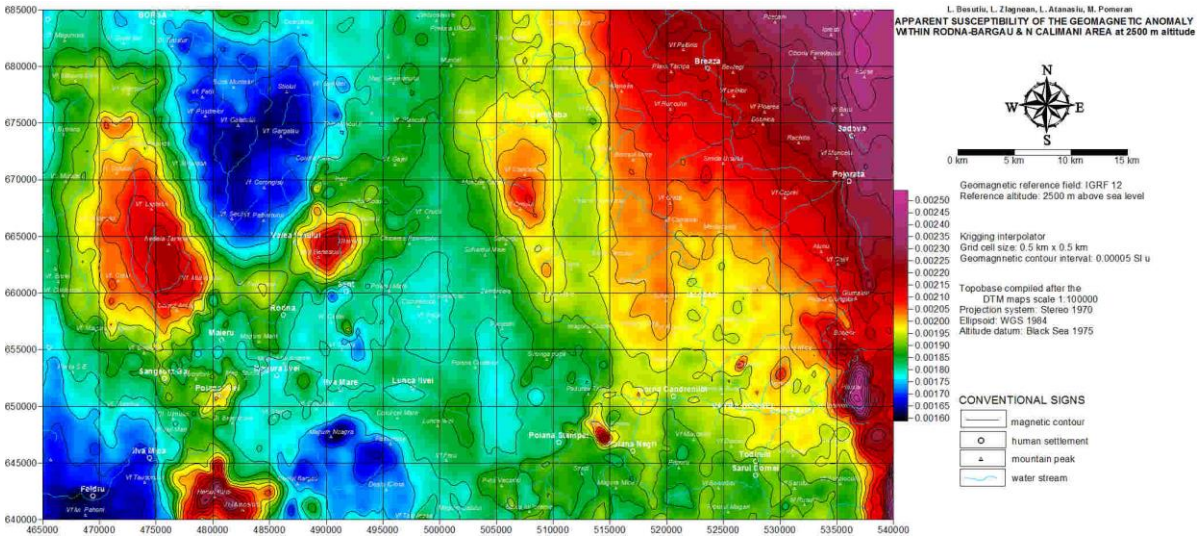

Fig. 4.2.3.2.1.15 Apparent geomagnetic susceptibility in the Rodna-Bârgău area

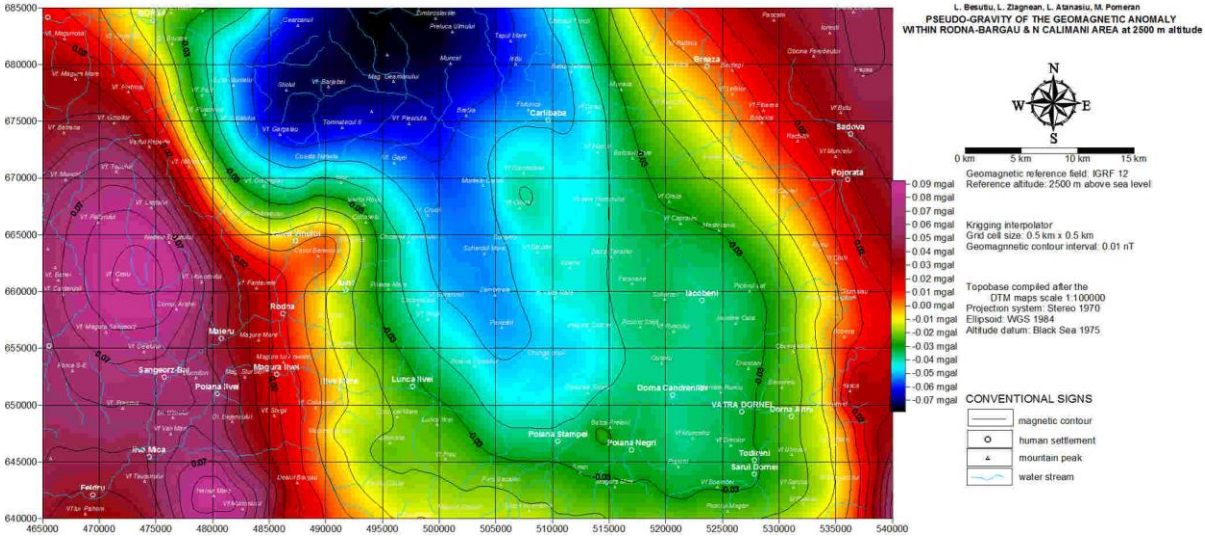

Fig. 4.2.3.2.1.16 Pseudo-gravity anomaly in the Rodna-Bârgău area

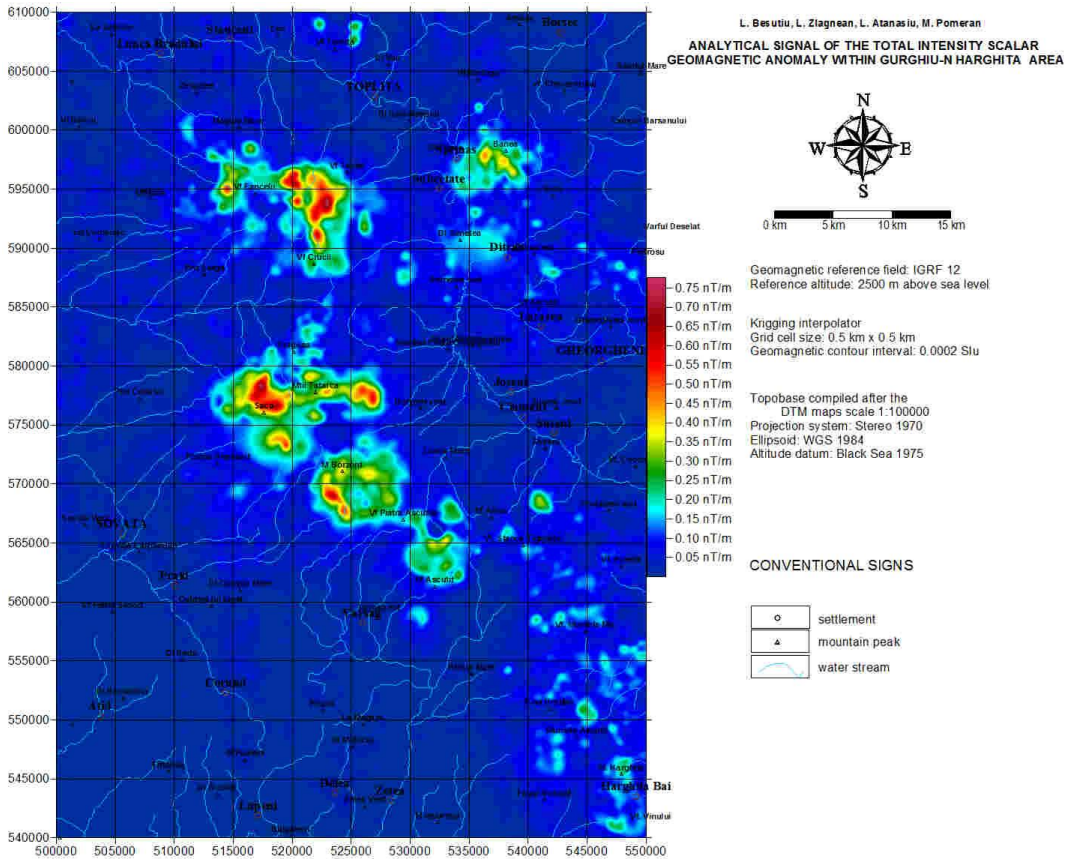

Fig. 4.2.3.2.1.17 Analytical signal of the reduced-to-pole geomagnetic anomaly in the Gurghiu area

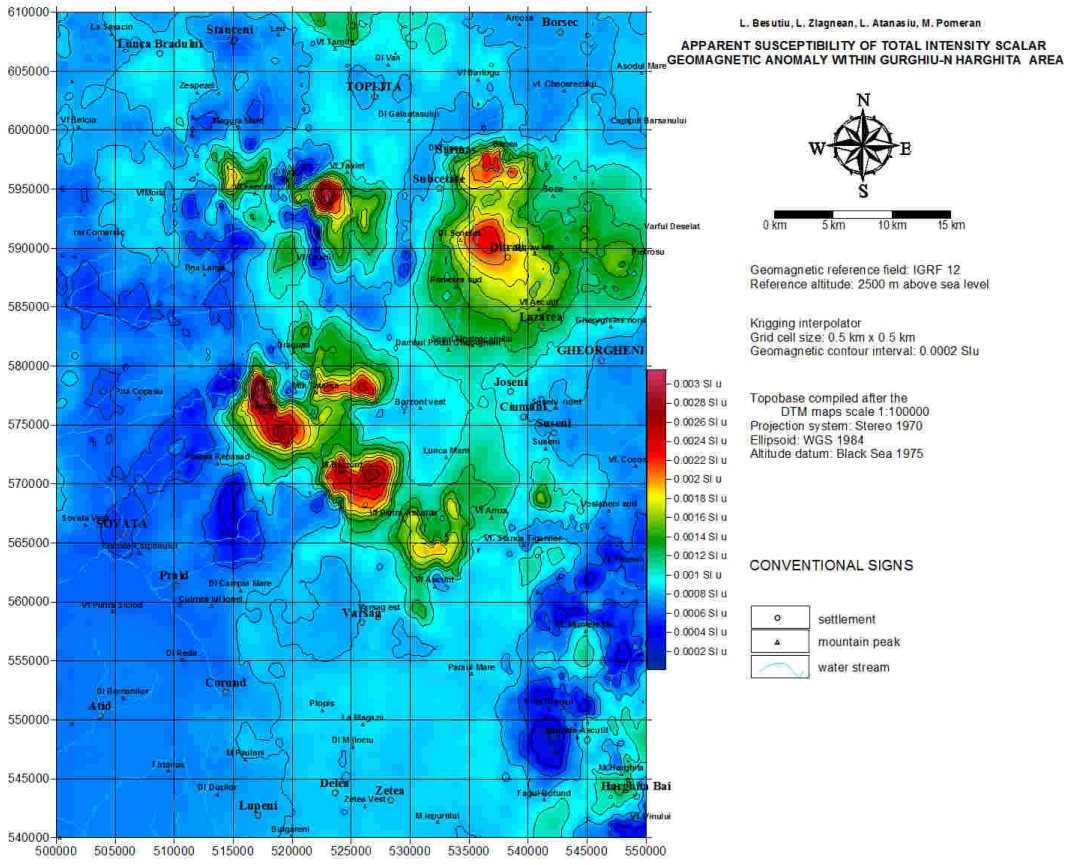

Fig. 4.2.3.2.1.18 Apparent magnetic susceptibility in the Gurghiu area

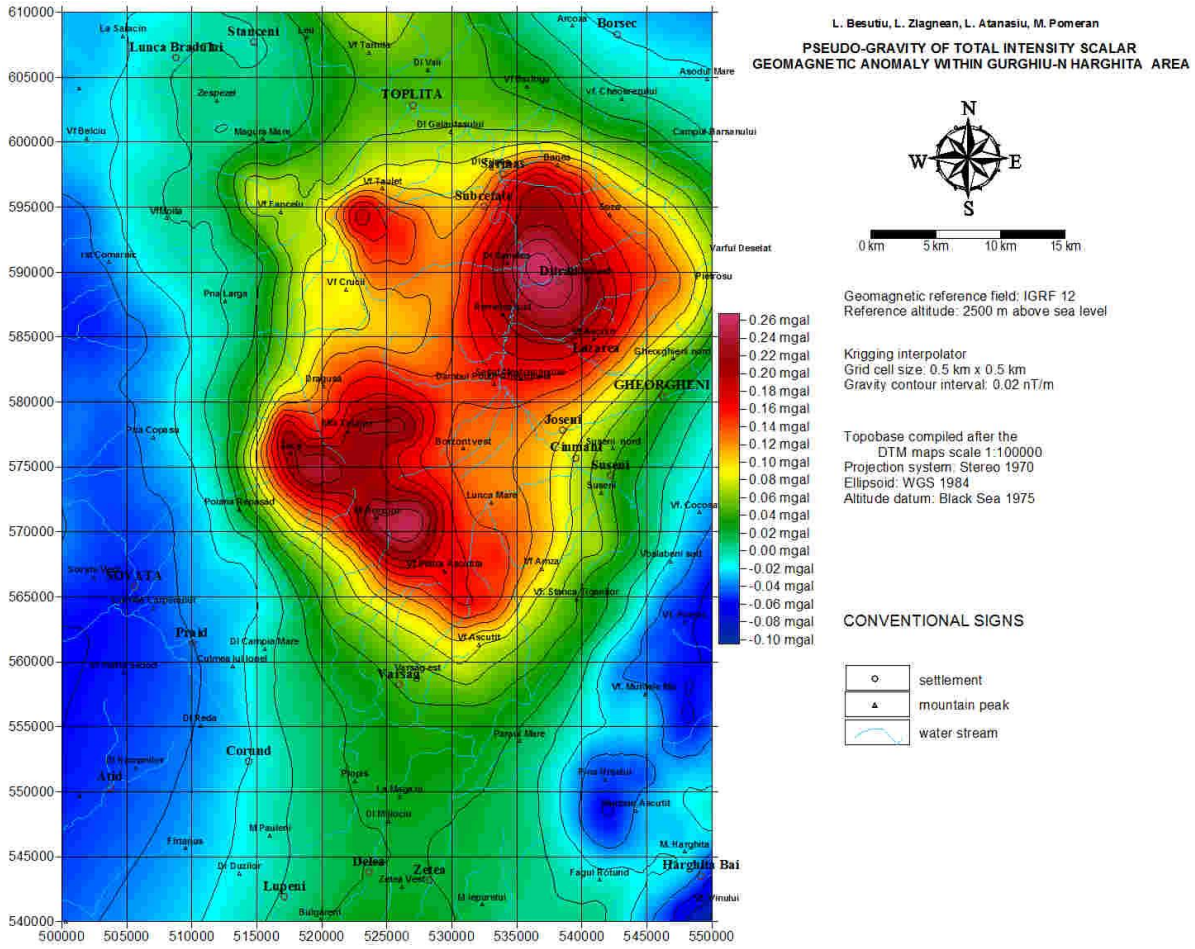

Fig. 4.2.3.2.1.19 Pseudo-gravity anomaly in the Gurghiu area

4.2.3.2.2. Filtered images of the gravity field

The following figures present the results obtained by filtering the Bouguer anomaly obtained within the investigated areas. The first order derivatives (vertical and horizontal gradient) and the analytical signal operators were applied relying on the capabilities of the OASIS application. Due to its appropriateness proved by comparing the gravity anomaly with topography, the 2670 kg/m^3 reference was used for obtaining the Bouguer signal.

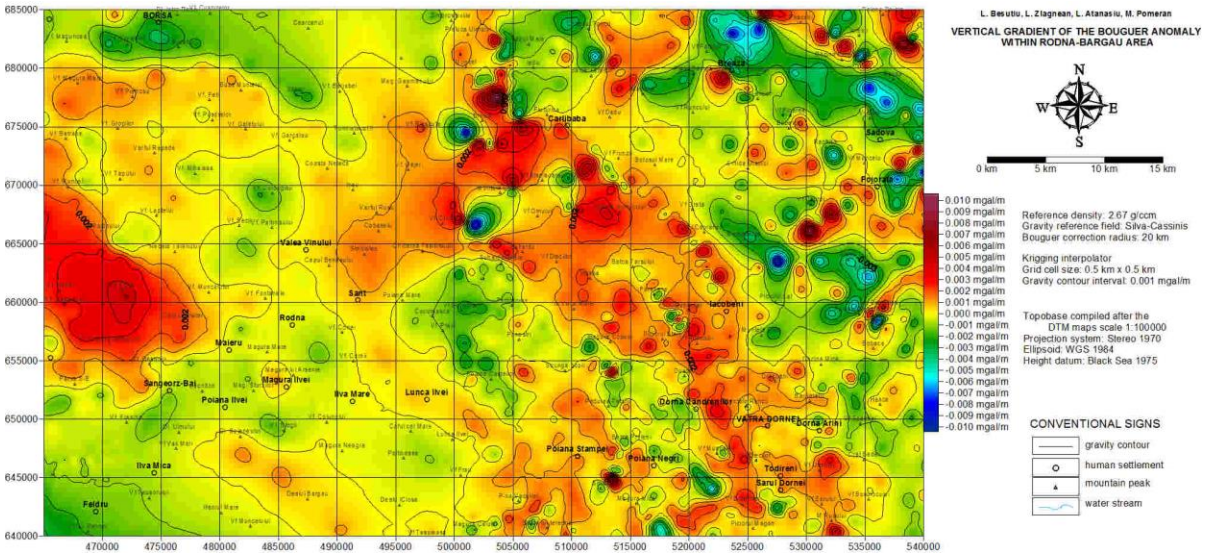

Fig. 4.2.3.2.2.1 Vertical gradient of Bouguer anomaly in the Rodna-Bârgău area

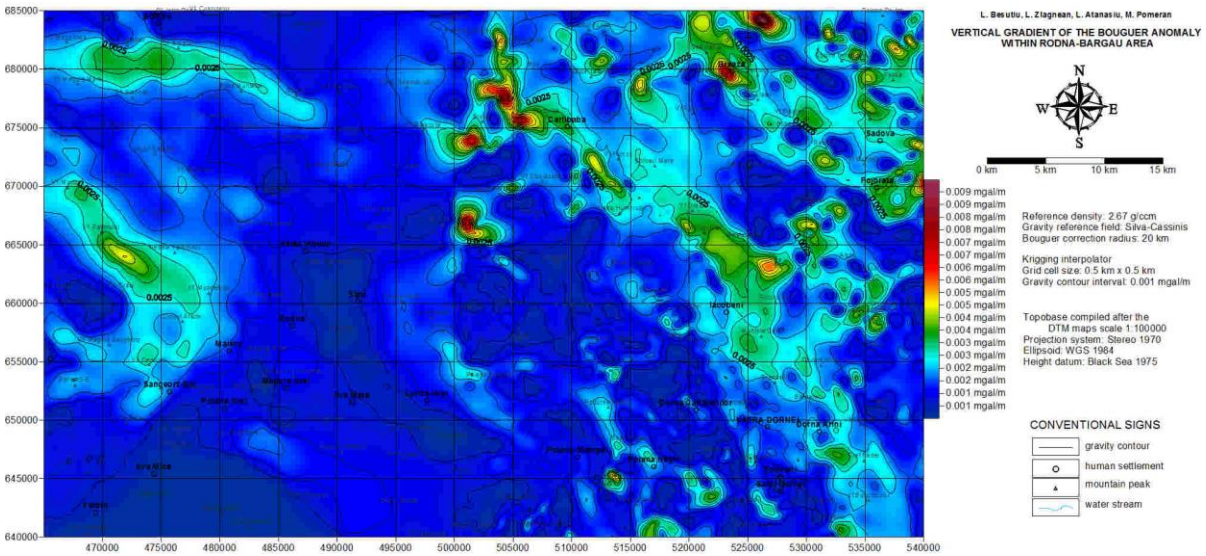

Fig. 4.2.3.2.2.2. Horizontal gradient of Bouguer anomaly in the Rodna-Bârgău area

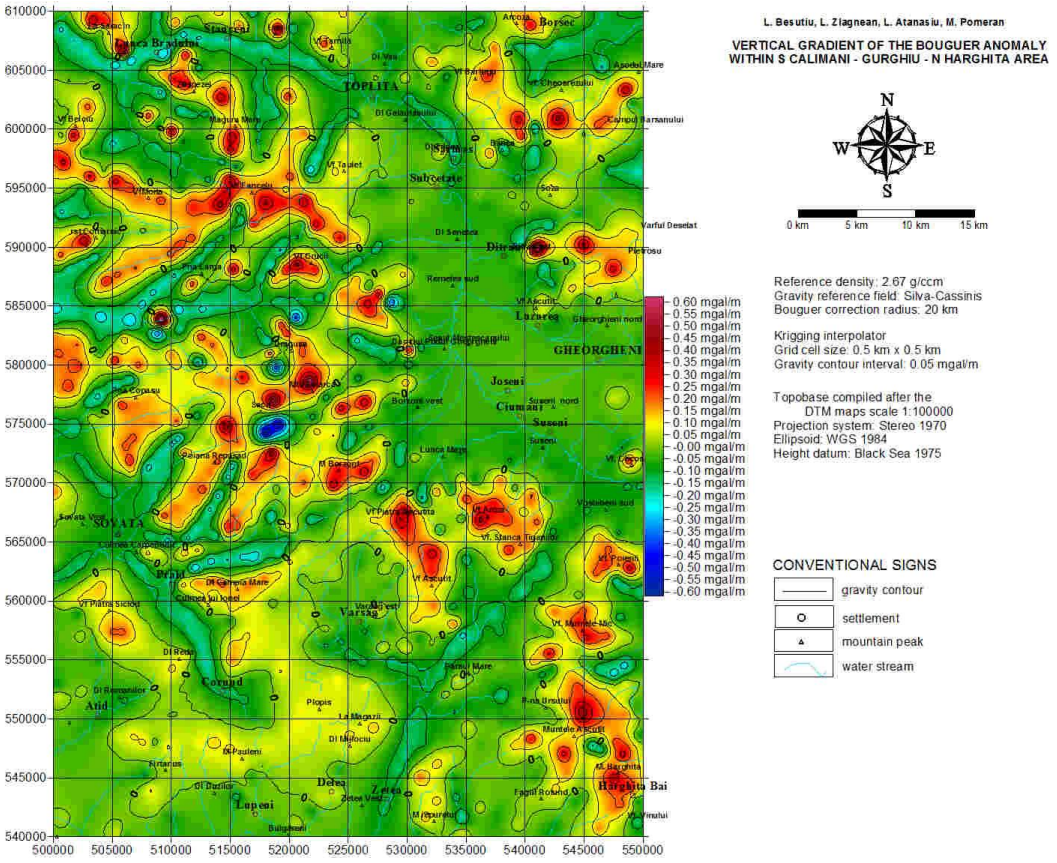

Fig. 4.2.3.2.2.3 Vertical gradient of Bouguer anomaly in the Gurghiu area

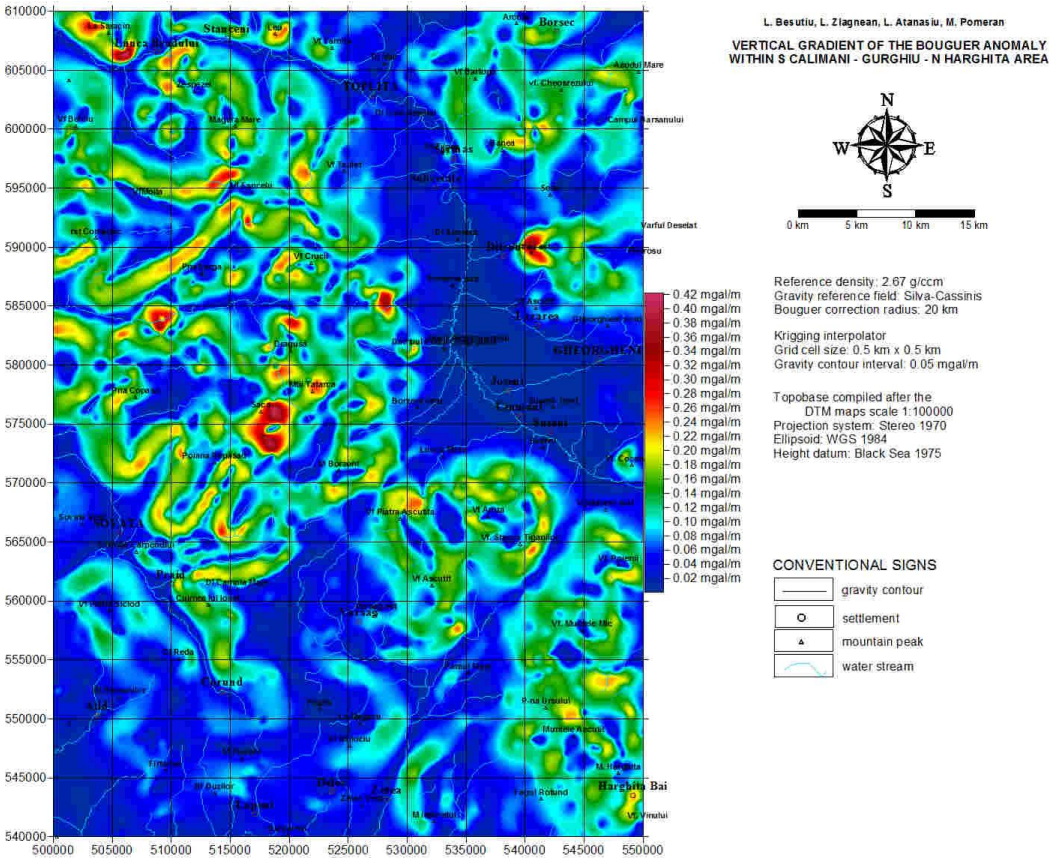

Fig. 4.2.3.2.2.4. Horizontal gradient of Bouguer anomaly in the Gurghiu area

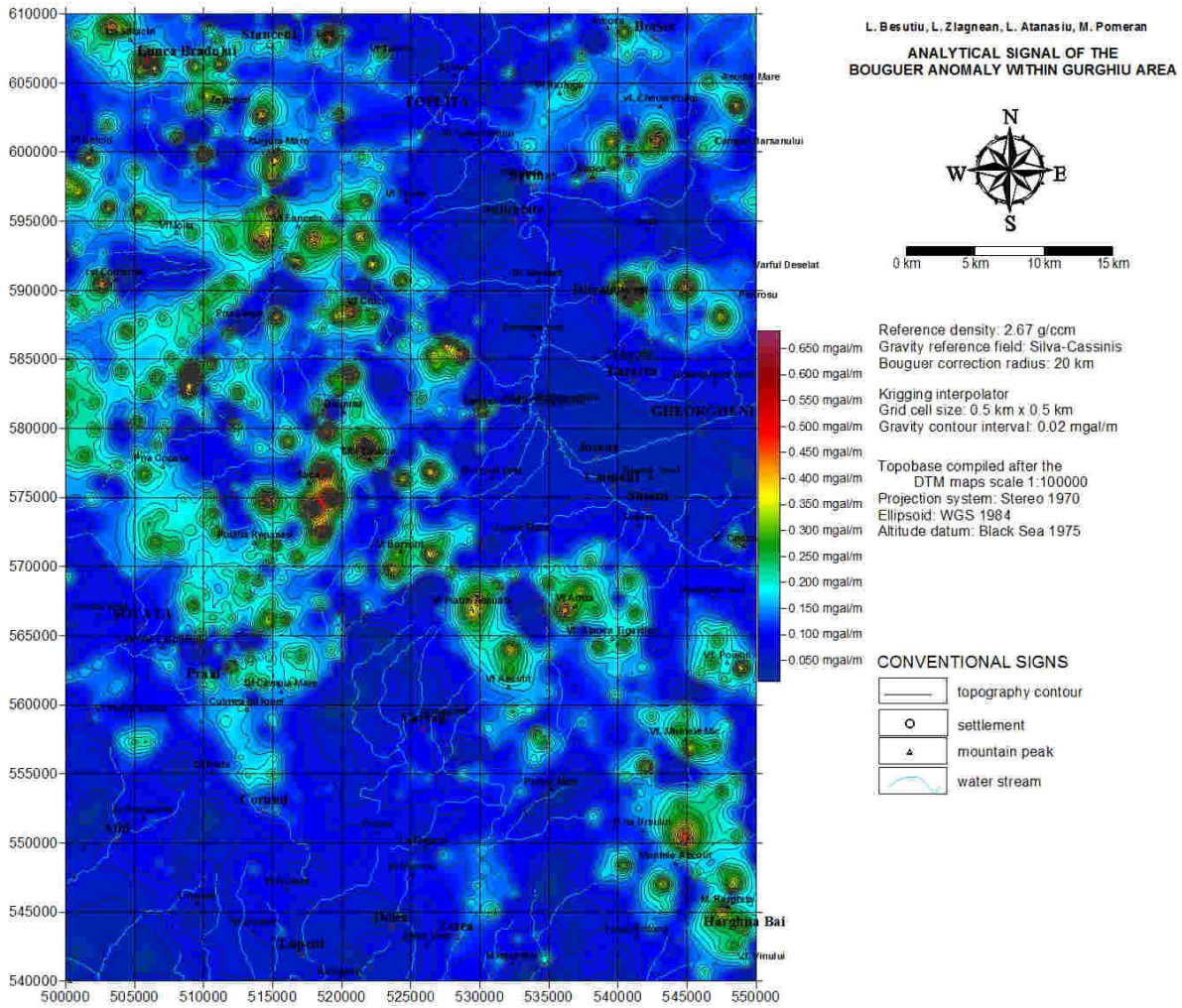

Fig. 4.2.3.2.2.5 Analytical signal of the Bouguer anomaly in the Gurghiu area

The analytical signal seems to reveal the presence of some conjugated fault systems (NW-SE and SW-NE) in the area, suggesting some major translations within NQECV transversal to the mountain chain but, in the absence of additional evidence, this remains a simple speculation.

4.2.3.3. Power spectra

In addition to the previously presented filtered maps, the power spectra of the both geomagnetic and gravity field within the investigated areas have been computed and are shown in the following figures along with depths to the major contrasts of physical properties that generate the anomalies.

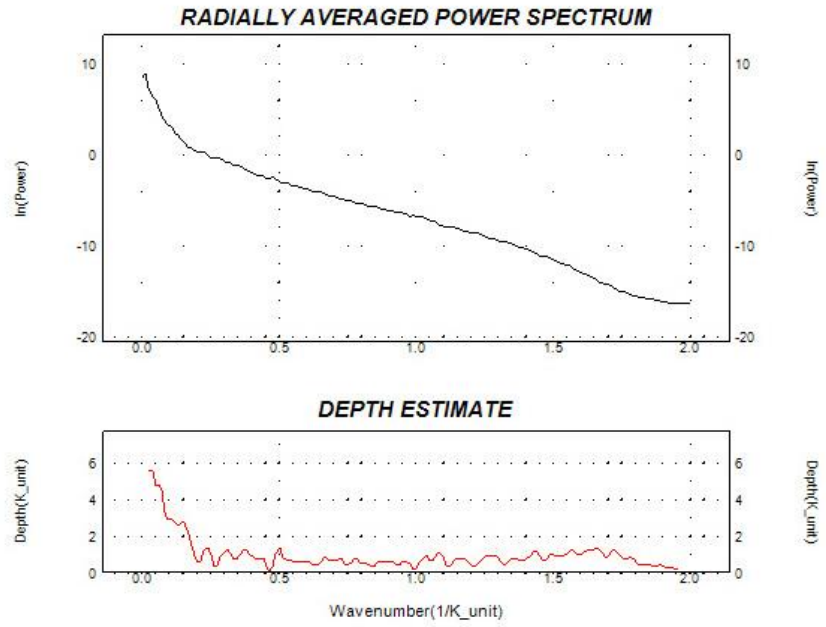

Fig. 4.2.3.3.1.1 Average radial power spectrum of the geomagnetic field and in depth sources distribution in the Rodna-Bârgău area

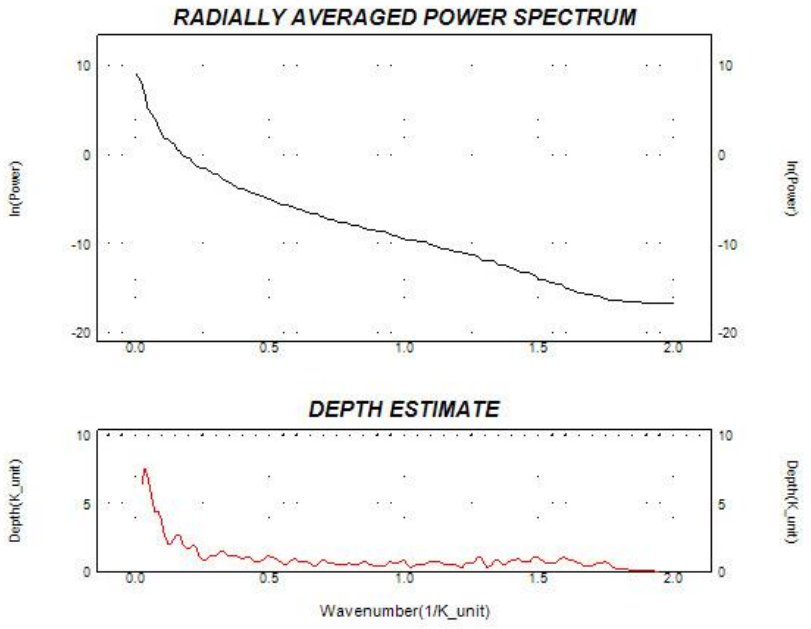

Fig. 4.2.3.3.1.2 Average radial power spectrum of the gravity field and in depth sources distribution in the Rodna-Bârgău area

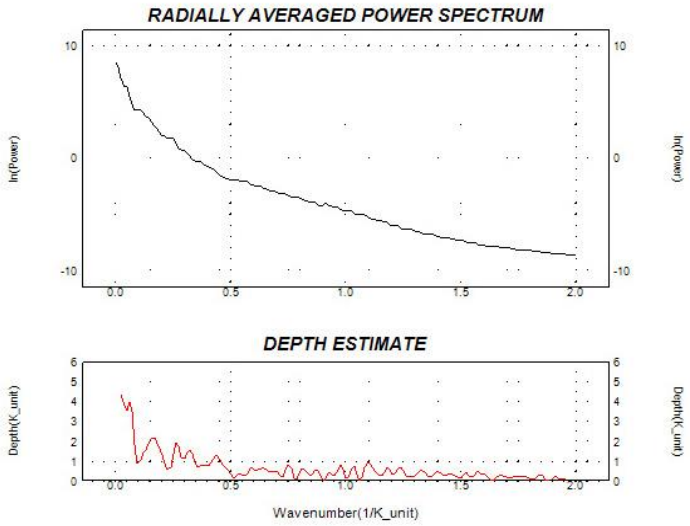

Fig. 4.2.3.3.2.1 Average radial power spectrum of the geomagnetic field and in depth sources distribution in the Gurghiu area

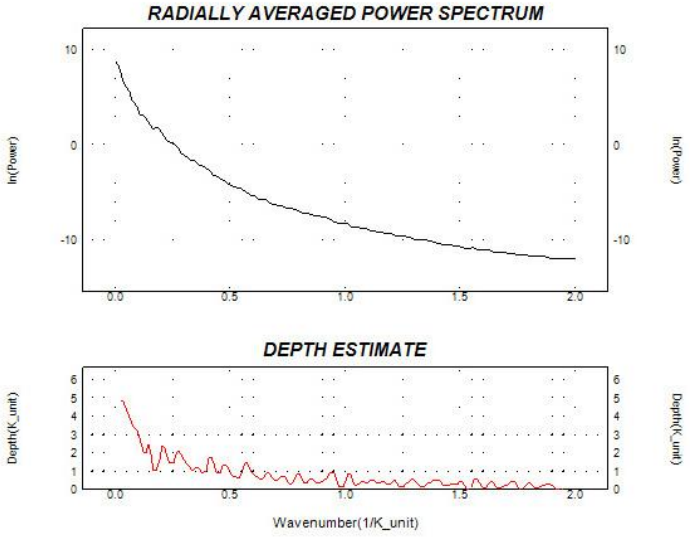

Fig. 4.2.3.3.2.2 Average radial power spectrum of the gravity field and in depth sources distribution in the Gurghiu area

4.2.3.4. Forward modelling: 2D models

In order to study the in-depth development of volcanic structures, several attempts for 2D numerical simulations in the northernmost part of the INSTEC perimeter have been made. Figure 4.2.3.4.1 presents the residual Bouguer anomaly, as obtained by removing a second order polynomial trend along with the location of interpretative lines along which attempts for 2D forward modelling have been made.

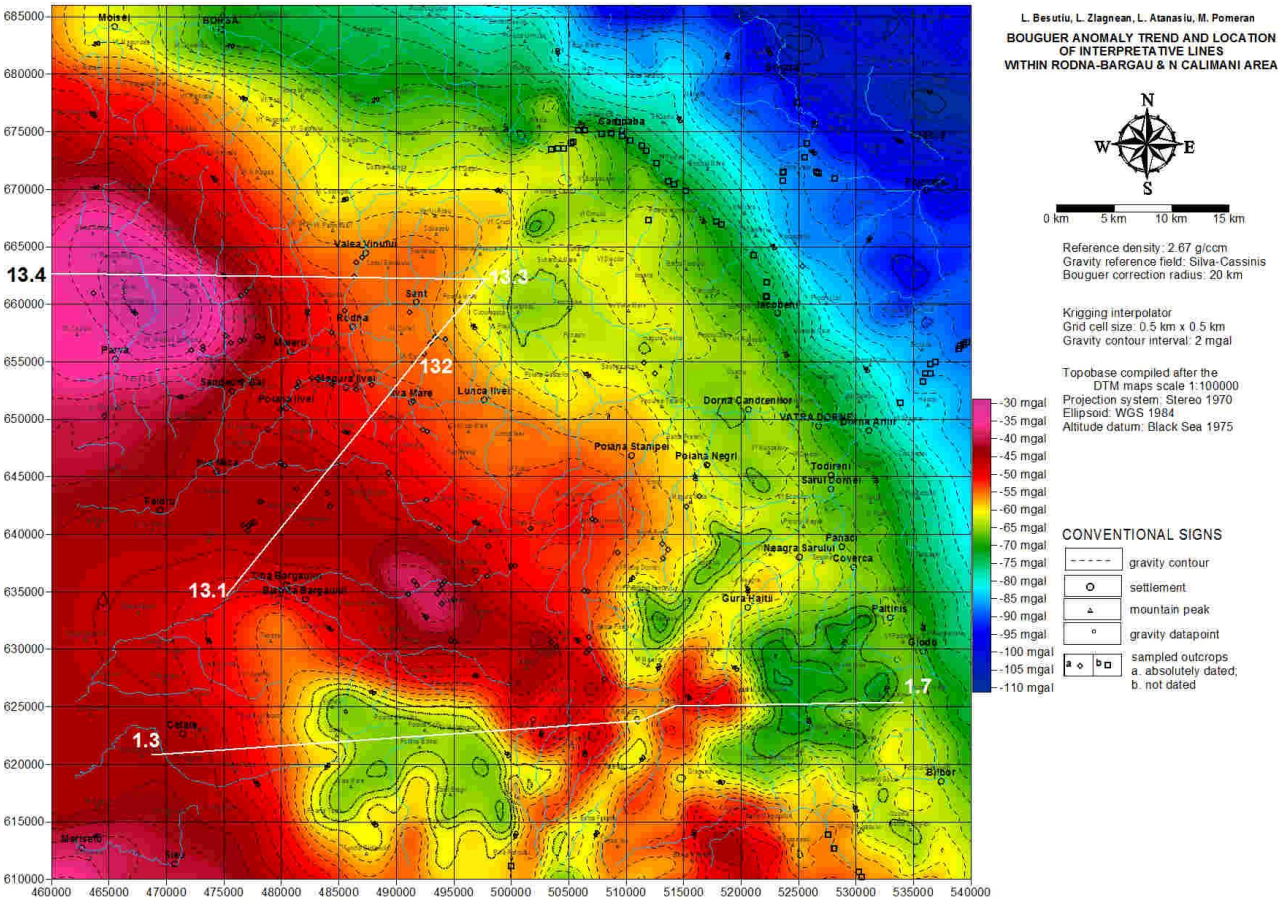

Fig. 4.2.3.4.1 Residual gravity anomaly and location of the interpretative lines in the Rodna-Bârgău and North Călimani Mts area

The GM-SYS 2D routine used for forward modelling is based on Talwani's algorithms. It has been run under OASIS platform to perform 2D modelling along the above-mentioned interpretative lines.

The initial models were built based on the current geological knowledge in the area, and physical properties of the main geological formations in the area (densities) have been added to complement the model. The first attempts did not show much agreement, but after several iterations, a good fit between observed and predicted

effect has been obtained (Fig. 4.3.4.2 - 4.2.3.4.4).

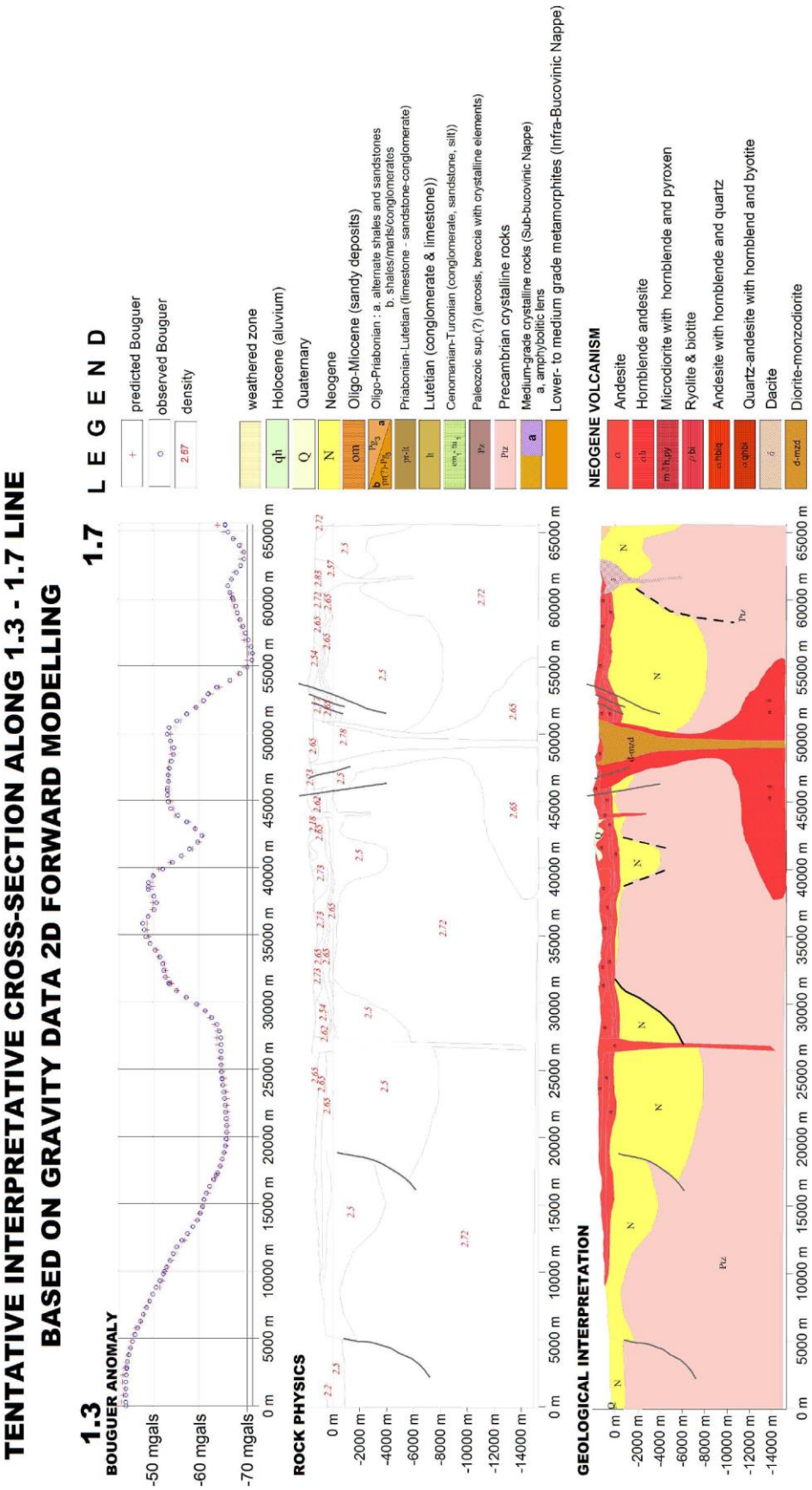

Fig. 4.2.3.4.2 Tentative interpretative cross-section along the 1.3 – 1.7 based on the 2D forward modelling of gravity data

Fig. 4.2.3.4.3 Tentative interpretative cross-section along the 13.1 – 13.3 based on the 2D forward modelling of gravity data

Fig. 4.2.3.4.4 Tentative interpretative cross-section along the 13.4 – 13.3 based on the 2D forward modelling of gravity data